ORIGINAL ARTICLE

Improving landings forecasts using environmental covariates: A case study on the Indian oil sardine (*Sardinella longiceps*)

Elizabeth Eli Holmes[1] | Smitha BR[2] | Kumar Nimit[3] | Sourav Maity[3] |
David M. Checkley Jr.[4] | Mark L. Wells[5] | Vera L. Trainer[1]

[1]Northwest Fisheries Science Center, National Marine Fisheries Service, NOAA, Seattle, WA, USA

[2]Centre for Marine Living Resources and Ecology, Ministry of Earth Sciences, Kochi, India

[3]Indian National Centre for Ocean Information Services, Ministry of Earth Sciences, Hyderabad, India

[4]Scripps Institution of Oceanography, University of California San Diego, San Diego, CA, USA

[5]School of Marine Sciences, University of Maine, Orono, ME, USA

Correspondence
Elizabeth Eli Holmes, Northwest Fisheries Science Center, 2725 Montlake Blvd E, Seattle, WA 98112 USA.
Email: eli.holmes@noaa.gov

Abstract

Commercial landings of sardines are known to show strong year-to-year fluctuations. A key driver is thought to be environmental variability, to which small forage fish are especially sensitive. We examined the utility of including environmental covariates in forecasts for landings of the Indian oil sardine using a long-term time series of quarterly catches. Potentially influential variables examined included precipitation, upwelling intensity, sea surface temperature (SST), and chlorophyll-a concentration. All of these have been shown to be important for oil sardine growth and survival, spawning and/or movement into the nearshore fishing regions. However, improving out-of-sample landings forecasts using environmental covariates has often proven elusive. We tested the inclusion of environmental covariates in forecast models using generalized additive models, which allow for non-linear responses, and dynamic linear models, which allow for time-varying responses. Only two environmental covariates improved out-of-sample prediction: the 2.5-year average regional SST and precipitation over land during June–July. The most significant improvement was with the SST covariate and post-monsoon landings with a 19%–22% reduction in mean-squared prediction error. Models with the second best covariate, monsoon precipitation over land, provided a 4%–8% reduction in prediction error. We also tested large-scale ocean climate teleconnection indices. One, an index of the Atlantic Multidecadal Oscillation, also improved out-of-sample predictions similarly to the multiyear average regional SST. The earth's changing climate is associated with both rapid warming in the Western Indian Ocean and changes to monsoon rainfall patterns. Our work highlights these as key variables that can improve forecasting of oil sardine landings.

KEYWORDS
Atlantic Multidecadal Oscillation, catch prediction, climate, dynamic linear modeling, GAM modeling, Indian oil sardine, remote sensing, sea surface temperature, Southeast Arabian Sea

1 | INTRODUCTION

Environmental variability is known to be a key driver of population variability for small forage fish, such as sardine, anchovy, and herring (Alheit & Hagen, 1997; Checkley et al., 2017; Cury et al., 2000). In particular, ocean temperature and upwelling dynamics have been shown to substantially affect the recruitment success and biomass of European and Pacific sardines (*Sardina pilchardus* and *Sardinops sagax*, respectively; Alheit et al., 2012; Garza-Gil, Varela-Lafuente, Caballero-Míguez, & Torralba-Cano, 2015; Jacobson & MacCall, 1995; Lindegren and Checkley, 2013; Lindegren et al., 2013; Rykaczewski & Checkley, 2008). The Indian oil sardine (*Sardinella longiceps* Valenciennes, 1847) is among the most commercially important fish resources along the southwestern coast of India—historically comprising up to 20% of the total marine fish landings in India (Vivekanandan et al., 2003). Similar to landings of other sardines, oil sardine landings show strong interannual fluctuations

with larger decadal booms and busts, but Indian oil sardine landings also have an unusually strong seasonal cycle driven by the summer monsoon. Landings peak in October–December, after the summer monsoon, and reach a nadir in April–June.

Two environmental variables, precipitation and coastal upwelling intensity, have been the focus of much research on the effect of the ocean environment on Indian oil sardine life history and landings. Precipitation during the summer monsoon and the day of monsoon arrival is thought to act as direct or indirect cues for spawning (Antony Raja, 1969, 1974; Jayaprakash, 2002; Murty & Edelman, 1966; Pitchaikani & Lipton, 2012; Srinath, 1998; Xu & Boyce, 2009). At the same time, intense monsoon rain over land causes high nutrient flux from rivers into the shallow nearshore regions which causes eutrophication and anoxia (Chauhan et al., 2011). The strong seasonal upwelling along the southwestern coast of India is also thought to be a key driver of variability in oil sardine abundance and catches. Coastal upwelling during the summer monsoon has dual effects: It

TABLE 1 Covariate models for the July–September (S_t) and October–March (W_t) landings. In the model (left) column, the first line is the environmental covariate. The response variable and the mechanism by which the covariate is postulated to affect catch is shown below the covariate (see Notes for the codes). The tests did not impose a direction (positive or negative) and some environmental covariates have been hypothesized to have both positive and negative impacts on oil sardines

Model	Description and justification
Jun–Jul and Apr–Mar ocean precipitation AF: S_t	Precipitation over the ocean may directly or indirectly prompt spawning, after which spent adults migrate inshore and are exposed to the nearshore fishery.
Jun–Jul land precipitation AF: S_t GS: W_t, W_{t+1}, S_{t+1}	Summer monsoon precipitation over land leads to high nutrient input from river discharge. At high levels, this leads to eutrophication and anoxia, which drives adults offshore away from the fishery. At moderate levels, this supports nearshore productivity.
Apr–Mar ocean precipitation SS: W_t, W_{t+1}, S_{t+1}	Spring precipitation is an indicator of climatic conditions during egg development, which affect spawning success and thus the cohort strength.
Jun–Sep upwelling AF: S_t GS+AF: W_t GS: W_{t+1}, S_{t+1}	Upwelling drives phytoplankton blooms which bring fish closer to the coast (and the fishery) and which promote larval and juvenile growth and survival. However extreme upwelling advects phytoplankton biomass offshore and brings hypoxic water to the surface.
Mar–May r-SST AF: S_t SS: W_t, W_{t+1}, S_{t+1}	Extreme pre-monsoon heating events drive mature fish from spawning areas, resulting in poor recruitment and fewer 0-year fish.
Oct–Dec ns-SST GS: W_t, W_{t+1}, S_{t+1}	October–December are the peak somatic growth months, and larval and juvenile growth and survival are affected by temperature in the nearshore feeding area.
Jul–Sep and Oct–Dec CHL AF: S_t GS+AF: W_t GS: W_{t+1}, S_{t+1}	Surface chlorophyll-a concentration is a proxy for phytoplankton abundance. Peak chlorophyll-a concentration is in July–September while October–December are critical months for juvenile growth and survival.
2.5-year average r-SST IA: S_t, W_t, W_{t+1}, S_{t+1}	Spawning, early survival, and recruitment depend on many cascading factors summarized by the average regional SST over the lifespan of an oil sardine.
ONI, PDO, AMO IA: S_t, W_t, W_{t+1}, S_{t+1}	The large-scale ocean climate has impacts on precipitation, SST, wind, currents and upwelling patterns in the southwestern Indian Ocean. These in turn have cascading impacts on spawning, early survival and abundance.
Sep–Nov DMI GS+AF: W_t GS: W_{t+1}, S_{t+1}	Negative DMI values in September–November are associated with anoxic events along the Kerala coast which drive fish offshore and reduce juvenile growth and survival.

Model codes: AF, availability to the nearshore fishery (movement inshore increases availability while movement offshore reduces availability); GS, growth and survival; IA, integrated abundance; SS, spawning success. Environmental covariates codes: r-SST, regional (0–160 km) sea surface temperature; ns-SST, nearshore (0–80 km) sea surface temperature; CHL, chlorophyll-a surface concentration; ONI, Oceanic Niño Index; DMI, Dipole Mode Index; PDO, Pacific Decadal Oscillation index; AMO, Atlantic Multidecadal Oscillation index.
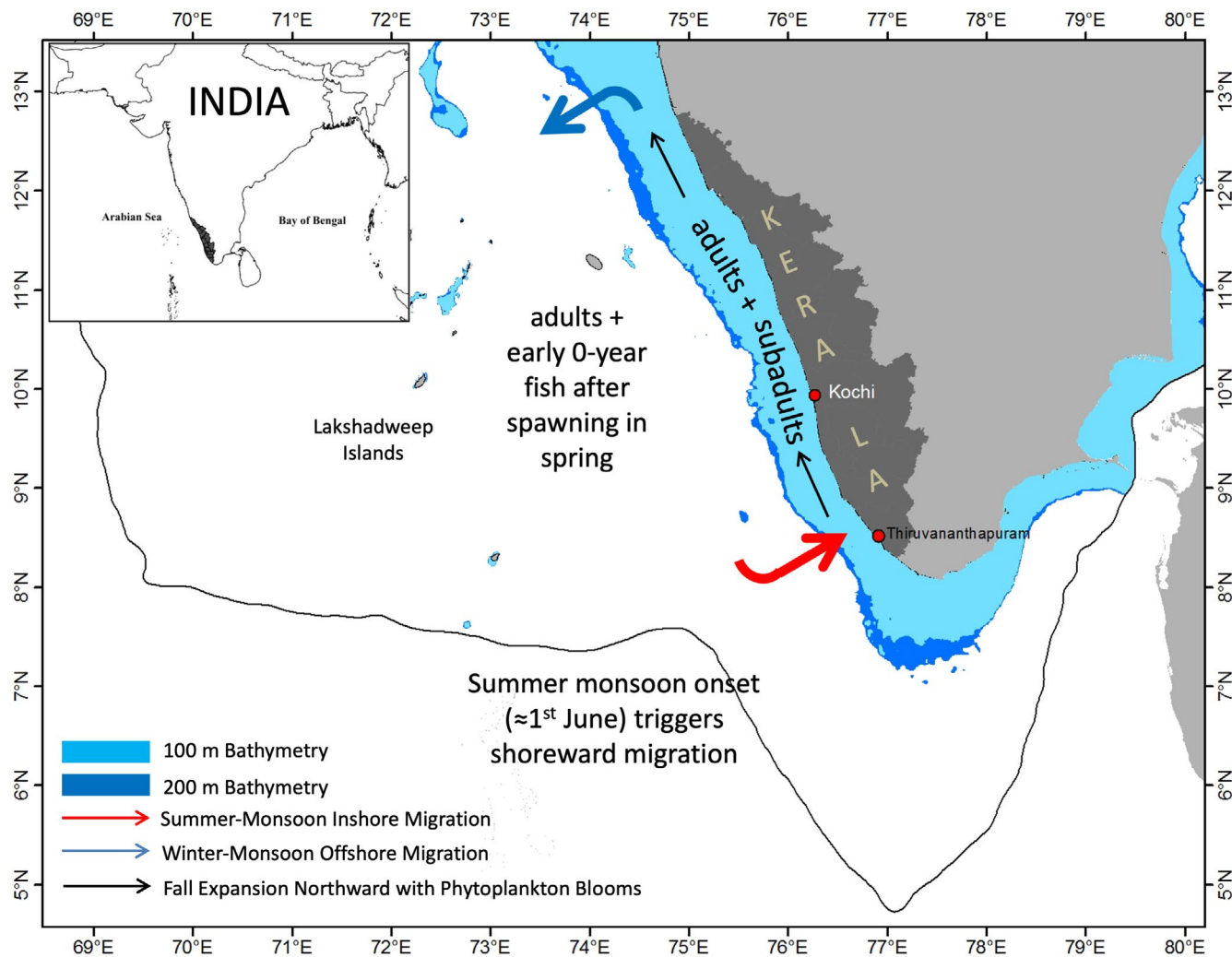
FIGURE 1 The study area, located off the southwestern coast of India. Kerala is shaded dark gray

fuels productivity but at high levels brings low oxygen water to the surface which can cause fish to move offshore where they are inaccessible to the fishery, while downwelling during spring is thought to promote the spring migration of adults into the nearshore where they are exposed to the fishery (Hamza et al., 2020). Correlations have been identified between landings and various indices of upwelling intensity (Hamza et al., 2020; Jayaprakash, 2002; Kripa et al., 2015; Longhurst & Wooster, 1990; Madhupratap, Shetye, Nair, & Nair, 1994; Murty & Edelman, 1966; Srinath, 1998; Thara, 2011); direct measures of upwelling-associated productivity (George et al., 2012; Madhupratap et al., 1994; Manjusha et al., 2013; Menon et al., 2019; Nair, 1952; Nair & Subrahmanyan, 1955; Piontkovski et al., 2014; Pitchaikani & Lipton, 2012); and the cold nearshore sea surface temperatures caused by upwelling (Annigeri, 1969; Pillai, 1991; Prabhu & Dhulkhed, 1970; Supraba et al., 2016).

In addition, to these regional environmental variables, climate teleconnection indices which capture large-scale ocean modes have also been examined for association with fisheries landings. Large-scale ocean climate modes, such as the El Niño–Southern Oscillation (ENSO), Indian Ocean Dipole (IOD) and Atlantic Multidecadal

Oscillation (AMO), have cascading effects on a variety of ocean conditions that affect small pelagics (Alheit et al., 2019; Alheit & Hagen, 1997; Bakun et al., 2008; Schwartzlose et al., 2010). Correlations have been found between ocean climate indices and oil sardine landings (Hamza et al., 2020; Rohit et al., 2018; Supraba et al., 2016), as well as with coastal anoxic events (Vallivattathillam et al., 2017) and chlorophyll blooms (Currie et al., 2013) in our study region.

This long and rich history of research on the Indian oil sardine provides a strong foundation for selecting and specifying the environmental factors that are most likely affecting the abundance and catchability of this important commercial species. In this paper, we study the utility of using these environmental covariates to improve out-of-sample landings predictions for the oil sardine, with the ultimate goal of improving short-term operational forecasts.

1.1 | Modeling and forecasting fishery landings

The modeling and forecasting of landings using time-series models have a long history in fisheries research (Cohen & Stone, 1987;

Farmer & Froeschke, 2015; Georgakarakos et al., 2006; Hanson et al., 2006; Lawer, 2016; Lloret et al., 2000; Mendelssohn, 1981; Nobel & Sathianandan, 1991; Prista et al., 2011; Stergiou & Christou, 1996), including for oil sardines (Sajna et al., 2019; Srinath, 1998; Venugopalan & Srinath, 1998). These models can be used to identify variables correlated with catch fluctuations and to provide short-term landings forecasts, which are useful for fishery managers (e.g., Farmer & Froeschke, 2015) and the fishing industry (e.g., Hanson et al., 2006; Schaaf et al., 1975).

One of the interesting puzzles in research on landings forecasting, and forecasting in general, is that it is often difficult to improve on simple low-dimensional autoregressive forecast models, that is a forecast that is a simple function of past values (Ward et al., 2014), and adding environmental covariates often degrades the forecast due to the added parameter estimation costs. The Indian oil sardine offers a unique opportunity to study the utility of environmental covariates for landings forecasts because there is extensive prior
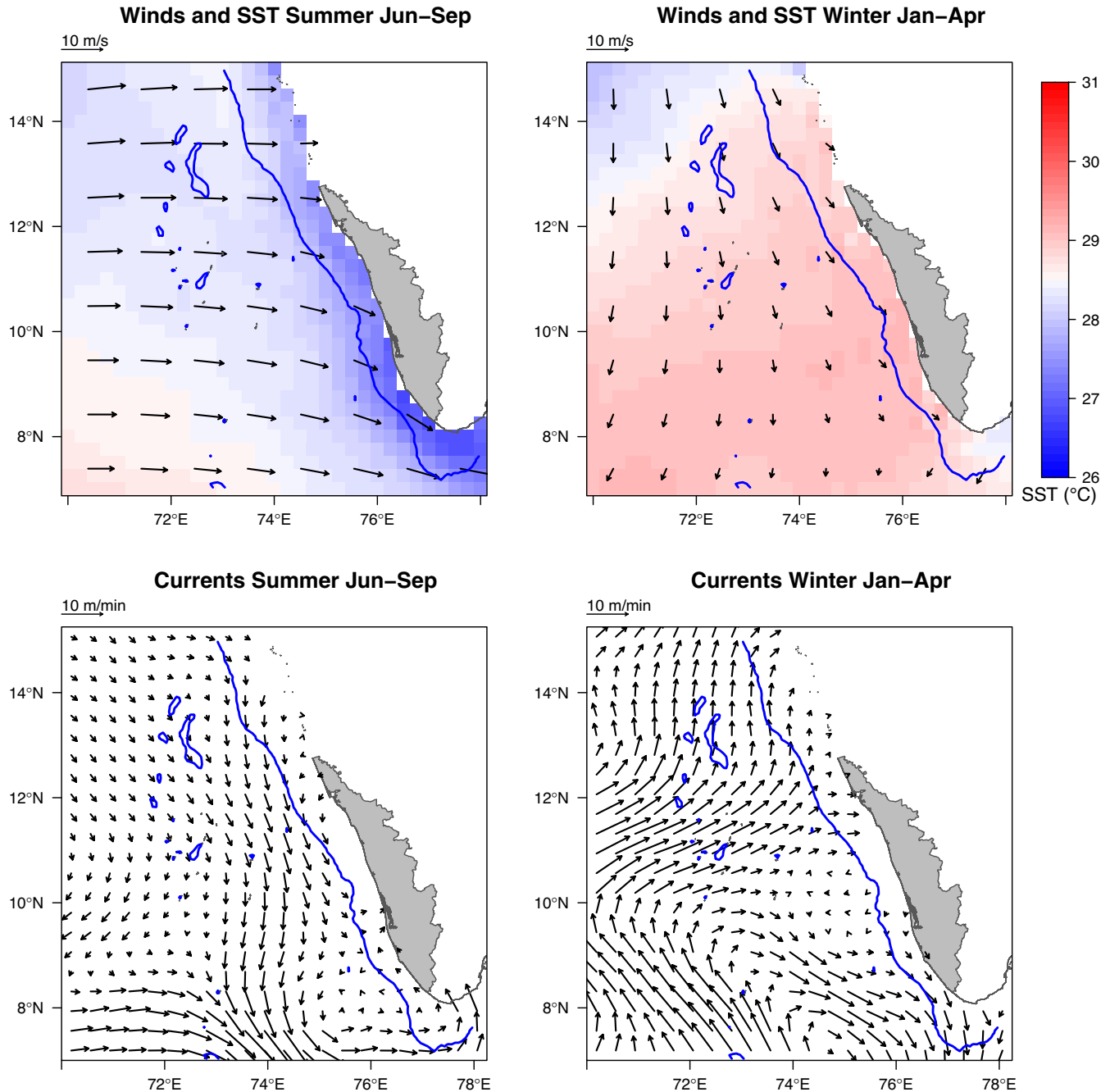

FIGURE 2 Seasonal average winds, sea surface temperature (SST) and currents during the summer monsoon versus the winter non-monsoon months in the study area. Winds and SST are from the Reanalysis Data ERA5 monthly product and averaged over 1979–2020. The bottom panels show the main seasonal currents near the study area: the West India Coastal Current going north in winter and south in summer and the Summer Monsoon Current going west to east near 8°N. The dark blue line is the 200m bathymetry line and the grey shaded region is Kerala

research of the environmental variables that influence the oil sardine's ocean environment and its exposure to the fishery and there is a long-term quarterly catch time series derived from a large-scale stratified statistical survey beginning in the 1950s (Srinath, Kuriakose, & Mini, 2005).

We first developed an autoregressive base catch model using only the prior-year landings to explain the current-year landings. Environmental covariates were then added to the base model, and we examined whether the covariate decreased the out-of-sample prediction errors and explained catch variability beyond that explained by the base model. We tested models with linear, non-linear and time-varying covariate effects. We focused primarily on covariates derived from remote-sensing products due to their broad spatial availability and temporal resolution, which make them practical for future operational forecasting efforts. The covariates were selected based on prior research supporting their correlation with nearshore productivity, juvenile growth and survival, and movement into or out of the nearshore (where they are exposed to the fishery); see Table 1.

1.2 | Study area

The study area is located off the Kerala coast of India (Figures 1 and 2), where the majority of Indian oil sardines are landed and where this species comprises about 40% of the marine fish catch (Srinath, 1998; Vivekanandan et al., 2003). It is in the Southeast Arabian Sea, one of the world's important seasonal upwelling zones (Habeebrehman et al., 2008; Madhupratap et al., 2001). The portion of the study area falling between 9°N and 13°N has especially intense upwelling in June–September due to the combined effects of wind stress (Figure 2) and remote forcing (BR, 2010; BR, Sanjeevan, Vimalkumar, & Revichandran, 2008; Shah et al., 2019). Upwelling gives rise to a strong temperature differential between the nearshore and offshore, and high primary productivity and surface chlorophyll (BR, 2010; Chauhan et al., 2011; Habeebrehman et al., 2008; Shafeeque et al., 2019). Primary productivity subsides after September, whereas mesozooplankton abundances increase and remain high in the post-monsoon period (Madhupratap et al., 2001).
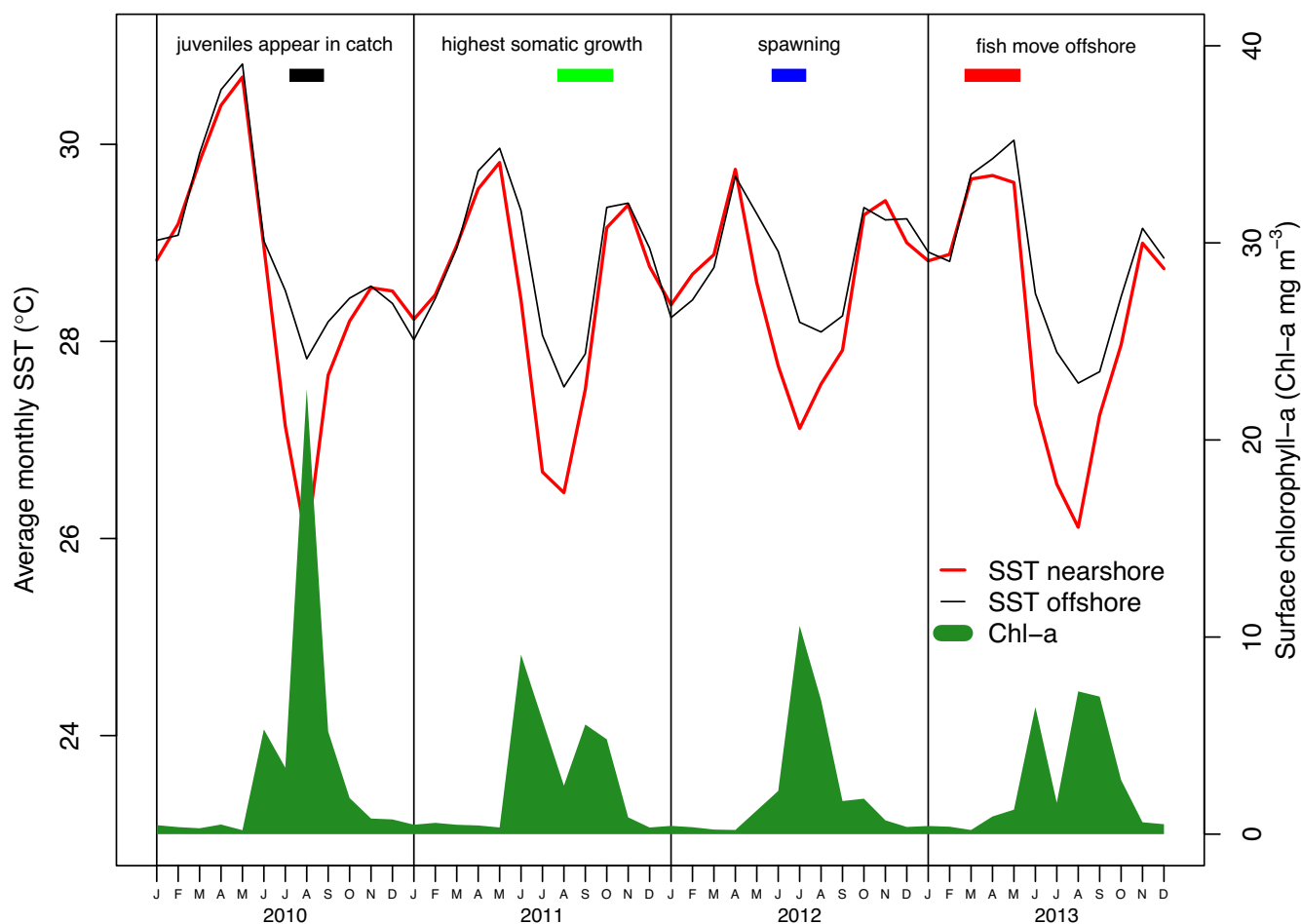

FIGURE 3 Key oil sardine life history events (top colored bars), overlaid on the monthly nearshore and offshore sea surface temperatures (SSTs; °C) and nearshore chlorophyll-a (Chl-a) concentrations (mg m^{-3})

1.3 | Oil sardine life cycle and fishery interaction

The Indian oil sardine fishery is restricted to the narrow strip of the western Indian continental shelf, <20 km offshore (Figure 1; Rohit et al., 2018). The yearly cycle begins with spawning in June and July, corresponding to the onset of the summer monsoon (Antony Raja, 1969) and much lower nearshore SSTs due to upwelling (Figure 3). Mature fish migrate from offshore to spawning areas (Antony Raja, 1964), and spawning begins when temperature, salinity, and food availability are conducive to larval survival (Jayaprakash & Pillai, 2000; Krishnakumar et al., 2008; Murty & Edelman, 1966; Nair et al., 2016). After an initial peak, spawning continues into September (Antony Raja, 1969; Hornell, 1910; Hornell & Nayudu, 1924; Prabhu & Dhulkhed, 1970). Both early- and late-spawning cohorts are evident in the length distributions of fish in the fall catch. After spawning, adults migrate closer to the coast (Figure 1), where the spent fish become exposed to the fishery and landings begin to increase. Catches during summer are dominated by these 1- to 2.5-year-old mature fish (Antony Raja, 1969; Bensam, 1964; Nair et al., 2016).

Spawned sardine eggs develop rapidly into larvae (Nair, 1959). The phytoplankton bloom that provides food for the larvae depends on nutrient influx from coastal upwelling and runoff from rivers during the summer and early fall (Shafeeque et al., 2019). Blooms start near the southern tip of India in June, then increase in intensity and expand northward with the peak of bloom intensity remaining south of 13°N, the northern end of Kerala (BR, 2010). Variation in the bloom initiation time and intensity leads to changes in the food supply, and thus in larval growth and survival and subsequent recruitment of 0-year sardines into the fishery (George et al., 2012). Oil sardines grow rapidly in the first few months of life, and spikes of 0-year fish from early spawning appear in the August and September catches in most years (Antony Raja, 1970; Nair et al., 2016). During late-summer and fall, both adult and juvenile sardines shoal and feed in the nearshore following the intense plankton blooms that develop off the Kerala coast. Oil sardines remain inshore to feed through winter and peak catches occur in October–December followed by January–March (Figure 4). These post-monsoon, October–March, catches are mixed age including fish from 0 to 2 years (Antony Raja, 1970; Nair et al., 2016; Prabhu & Dhulkhed, 1970; Rohit et al., 2018). In March–May, the sardines move offshore to deeper water where they are no longer available to the fishery, landings consequently decline (Figure 4), and the seasonal cycle begins anew.

Landings are products of abundance, effort, and catchability (i.e., availability to the nearshore fishery). For much of the period of our study, the Indian oil sardine fishery was largely unregulated and has been a nearshore fishery dominated by small boats. For this time period, the yearly landings are often assumed to reflect total
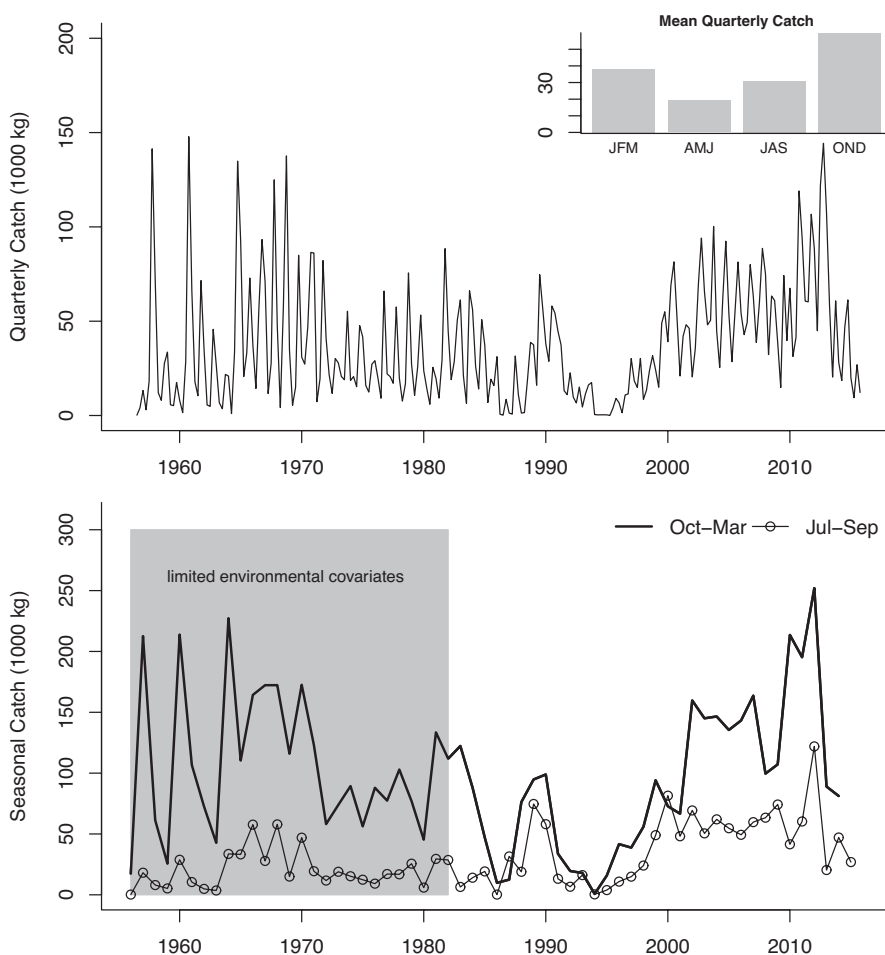

FIGURE 4 Top panel: Quarterly catch data for 1956–2015 from Kerala. Note that the fishery is closed July 1–mid-August, meaning that the quarter 3 catch represents only 1.5 months. Mean catches in quarters 1–4 were 38, 19.2, 30.9, and 59.9 metric tons, respectively. Bottom panel: The seasonal time series (July–September and October–March catch) used in the paper

abundance for species- and fishery-specific reasons (cf. Kripa et al., 2018). The ring seine was introduced in this fishery in the 1980s (Das & Edwin, 2018), but widespread mechanization of the fleet is a recent development. Fishers with small boats with no refrigeration have limited ability to target stock, at least not to the degree that landings would remain constant as abundance declines, as can

be seen with a large, mobile, highly mechanized fleet. The fishery is unregulated, except for a brief closure during the summer monsoon, and thus landings are not affected by area closures or catch limits. Finally, the fishery is dispersed along the entire coastline, rather than being focused from a few large ports. Thus, the relationship between landings and abundance can be assumed to be strong for
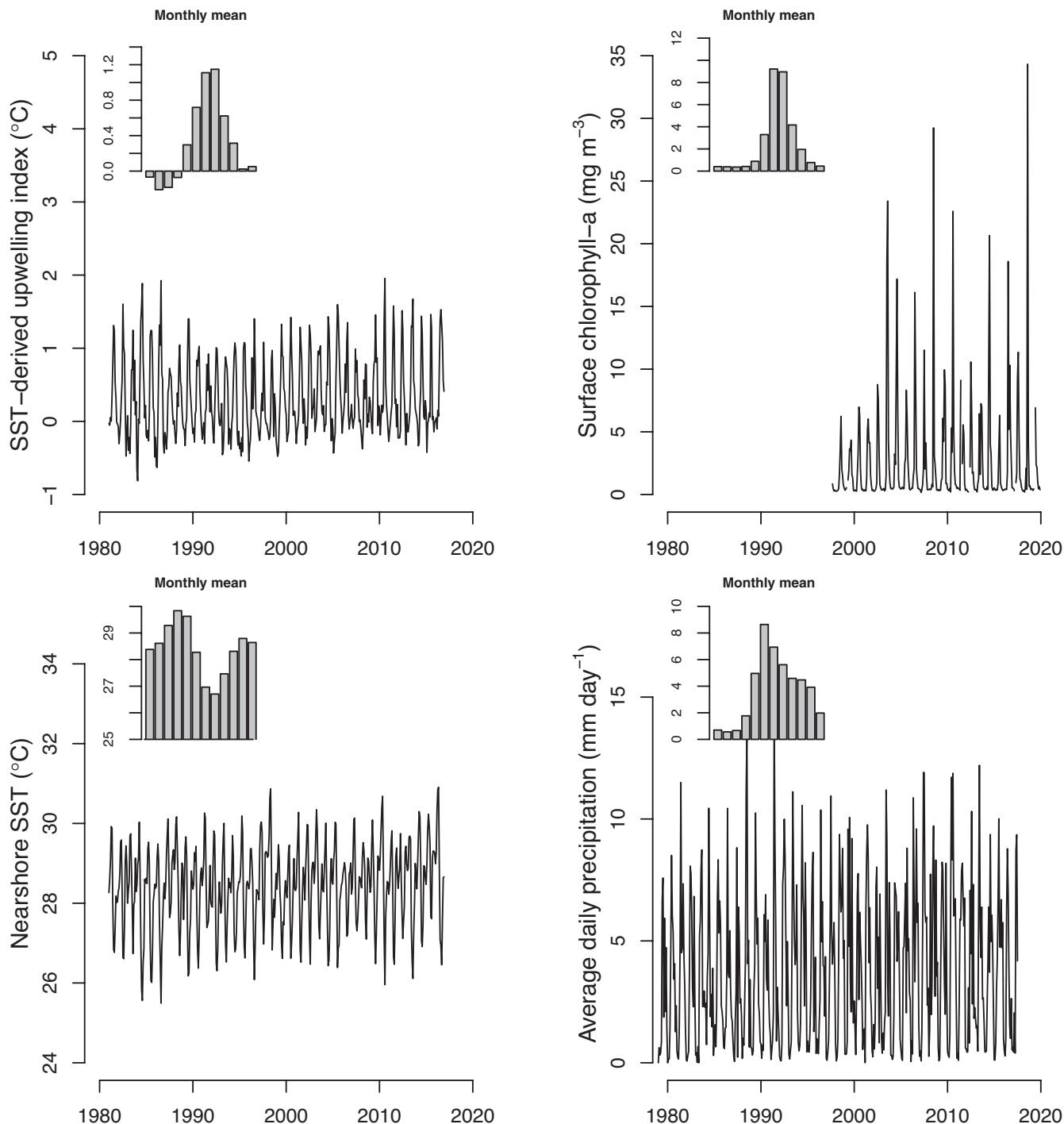

FIGURE 5 Four of the remote-sensing covariates used in the analysis. All data are monthly averages. The upwelling index was defined as the difference between the nearshore and 3° longitude offshore sea surface temperatures (SSTs). Surface chlorophyll-a data are available only from September 1997 onward. SSTs were obtained from Advanced Very High Resolution Radiometer (AVHRR) products which provide high resolution nearshore measurements

our data set and comparison of the landings to the available catch-per-unit effort (hours fishing) data shows high correlation (Hamza et al., 2020). Seasonal variation in the oil sardine catch is affected both by movement of fish in and out of the nearshore (Figure 1) and recruitment of juvenile fish to the fishery.

2 | MATERIALS AND METHODS

2.1 | Sardine landing data

The Central Marine Fisheries Research Institute (CMFRI), Kochi, India, has collected quarterly fish landing data along the country's southwestern coast since the early 1950s using a stratified multi-stage sampling design which accounts for the different boat and gear types (Srinath et al., 2005). We used CMFRI data from the Indian state of Kerala (Figure 1), which has the longest and most complete time series and where the overwhelming majority of oil sardines are landed (Figure 4). Quarterly oil sardine landings data (in metric tons) for all gear types used in Kerala were obtained from CMFRI reports (1956–1984) and online databases (1985–2015). See the Supplemental Information: Data sources and raw data. These data were log transformed to stabilize variance and to facilitate additive modeling.

2.2 | Environmental data

We analyzed monthly composites of SST, chlorophyll-a concentration, precipitation, upwelling indices derived from SST and winds, and ocean climate indices (Figures 2 and 5). For each covariate, specific months (seasons) were used corresponding to different aspects of oil sardine life history and its interaction with the nearshore fishery. These are summarized in Table 1. See the Supporting Information: Data sources and raw data for all environmental data details, sources and code to compute metrics and download the data.

We tested SST (°C) averaged between 8° and 13°N in the nearshore (within 1° of the coast) in June–September (summer monsoon period of peak upwelling, spawning, larval growth, and survival) and October–December (peak juvenile somatic growth). SST in the current year could affect landings by causing fish movement in and out of nearshore and/or affecting juvenile abundance while prior-year effects would arise via effects on cohort strength. We tested SST regionally, between 8° and 13°N and up to 2° offshore, in the spring (March–May) and over the prior 30 months (January t-2 to June t). The former may affect egg development, spawning, and inshore migration timing thus affecting both current and future year abundance and availability to the fishery. The latter integrates effects of SST over the average sardine life span and has been shown to be correlated with recruitment in other sardine species (Checkley et al., 2017). For our SST source, we used the Daily Optimum Interpolation (OI), version 2.1 data set by the Group for High Resolution Sea Surface Temperature (GHRSST). This data set uses Advanced Very

High Resolution Radiometer (AVHRR) data, which provides accurate nearshore SST values, and interpolates to fill in gaps in the AVHRR data. See the section on comparison of SST products in the Supplemental Information: Full model tests and diagnostics. We used OI SST for all the main analyses which use landings data after 1981. For our analysis of the effect of the regional- (as opposed to near-shore-) SST prior to 1981, we used the International Comprehensive Ocean-Atmosphere Data Set (ICOADS) SST product, available from 1960. The nearshore (<80 km) ICOADS SST measurements are not as accurate as AVHRR and could not be used for our covariates involving nearshore SST, such as the nearshore-offshore SST differential.

The strength of upwelling during the summer monsoon June to September has been widely studied for its effects on coastal productivity and coastal anoxia. The upwelling dynamics in our study area are unusual in that remote oceanographic forcing is an especially important driver of the seasonal upwelling intensity in combination with forces from local wind stress (BR, 2010; BR et al., 2008; Rao et al., 2008). We used a variety of SST- and wind-based indices that have been used in recent papers on upwelling dynamics off the southwest coast of India. We tested both current-year effects which could arise via effects on abundance or lower catchability due to movement offshore to avoid nearshore anoxia and prior-year effects which would arise via cohort strength in the prior year. The first index was the SST differential between nearshore and 3° longitude offshore, based on Naidu et al. (1999) and BR et al. (2008). This index has a strong temporal association with chlorophyll-a blooms (Figure 3) and is able to measure upwelling arising due to both remote-forcing and local wind stress. SSTs were obtained from the AVHRR remote-sensing data set described above. The second index was the Ekman Mass Transport (EMT; kg m^{-1} s^{-1}) perpendicular to and within 2° longitude of the coast (Schwing et al., 1996; Shafeeque et al., 2019). The third index was the Ekman Pumping (W_e; m s^{-1}) at the tip of India (Shah et al., 2019). EMT and W_e are computed from surface winds and capture upwelling due to local wind stress. We used the Reanalysis Data ERA5 monthly 10 m winds from the European Centre for Medium-Range Weather Forecasts. See the Supplemental Information: Ekman Mass Transport and Pumping Calculations for the equations and code for computing EMT and W_e from surface winds and for a comparison of the ERA5 winds to other remote-sensing wind products.

Precipitation over land and over the ocean during the summer monsoon (June to September) and spring (April to May) were tested in both the current and prior year. Precipitation over land leads to river discharge, which has various and large influences, positive and negative, on the nearshore ocean environment. Precipitation data were obtained from two sources: monthly precipitation (in millimeters) over Kerala, obtained with land-based rain gages and available from the Indian Institute of Tropical Meteorology from 1956; and daily precipitation (averaged monthly) over the ocean from remote-sensing (via the NOAA Global Precipitation Climatology Project). From the latter, we extracted data for the 2.5°× 2.5° box defined by latitude 8.75–11.25°N and longitude 73.25–75.75°E off the Kerala coast. The land and nearshore ocean precipitation data are correlated (Supporting Information; Figure S6).

Satellite-derived chlorophyll-a data are only available since September 1997 and were not the focus of our analysis due to low sample size, however, were included for preliminary study. We examined current and prior-year effects of chlorophyll-a concentration in the summer monsoon (June to September) period of peak upwelling and peak blooms (Figure 3) and in the October to December period of peak juvenile somatic growth. For chlorophyll-a concentration (mg m^{-3}), we used the R2018.0 and R2018.1 products developed by the NASA Ocean Biology Processing Group of the Ocean Ecology Laboratory.

We used four climate indices that have been found to correlate with either oil sardine landings, coastal anoxia, chlorophyll-a concentration, or upwelling intensity in recent studies: Oceanic Niño Index (ONI), the Dipole Mode Index (DMI), the Pacific Decadal Oscillation (PDO) index, and the Atlantic Multidecadal Oscillation (AMO) index. The ONI is a measure of the SST anomaly in the east-central Pacific and a standard index of the ENSO cycle. The DMI is defined by the SST anomaly difference between the western and southeastern Indian Ocean and is an index for the Indian Ocean Dipole cycle. It has been shown to predict anoxic events in our study area (Vallivattathillam et al., 2017) and seasonal chlorophyll-a blooms in the southeastern Indian Ocean (Currie et al., 2013). The PDO and AMO indices are measures of the SST anomalies in the North Pacific and North Atlantic Oceans, respectively. Hamza et al., (2020) found significant correlation between PDO and AMO indices and multiyear fluctuations in oil sardine landings. For ONI, PDO, and AMO indices, we created an annual covariate from the average July t-1 to June t values. The yearly average was computed this way so that it would not overlap with the July–September catch that we are forecasting.

2.3 | Base catch models

The first step in our analysis was to determine our base models for current catch as a function of past catch. We modeled July–September (late-monsoon) and October–March (post-monsoon) catches separately, for biological and statistical reasons. Unlike the October–March catch, the July–September catch contains mainly mature spawning-age fish, is affected by the monsoon fishery closure, and is affected by the timing of post-spawning movement inshore which exposes fish to the fishery. The covariates that affect the timing of spawning and post-spawning inshore movement may differ from those that affect egg, larval and juvenile survival, and nearshore shoaling (and thus the size of the October–March catch). Separating the catches into seasons, and analyzing annual series, eliminated the confounding influence of seasonality and permitted a focus on year-to-year variability rather than the seasonal cycle. Although adults in July–September would be those that spawn the 0-year fish in the October–March catch, the July–September catch in year t was not used as a predictor for October–March catch in year t. The focus of our work is the study of forecasting performance; the July–September catch numbers would not be available by October (the quarter immediately after).

We found little support for autoregressive errors, that is, Autoregressive Integrated Moving Average (ARIMA) models with moving average (MA) components, based on diagnostic tests of the residuals and model selection. The best-supported ARIMA models were simple AR models ($x_t = \alpha + \beta x_{t-1} + \epsilon_t$) where the error-term ϵ_t was temporally independent. Similar lack of strong autocorrelation in residuals has been found in other studies using ARIMA catch models for small pelagics (Stergiou & Christou, 1996). We thus used AR-only models; however, we tested linear and non-linear models with generalized additive models (GAMs; Wood, 2017) of the form $x_t = \alpha + s(x_{t-1}) + \epsilon_t$, where $s()$ is a non-linear spline smoothing function, and time-varying linear models with dynamic linear models (DLMs) of the form $x_t = \alpha_t + \beta_t x_{t-1} + \epsilon_t$. GAMs enable modeling of the effect of a covariate as a flexible non-linear function, and DLMs allow the effect of the covariate to vary over time. Our GAM approach is analogous to that taken by Jacobson and MacCall (1995) in a study of the effects of SST on Pacific sardine recruitment.

We explored four classes of base catch models: a naïve (null) model, linear regressive models with 1–2 years of prior catch data, DLMs (using the MARSS package in R; Holmes et al., 2012), and GAMs (using the mgcv package in R; Wood, 2011). We fit GAMs with smooth terms represented by penalized thin-plate regression splines and fixed the smoothing term at an intermediate value (sp = 0.6) to obtain smooth responses, as multimodal or overly flexible response curves would not be realistic for our application. The catch models were:

- naïve (null): $\ln(C_{i,t}) = \ln(C_{j,t-1}) + \epsilon_t$
- biased random walk: $\ln(C_{i,t}) = \alpha + \ln(C_{j,t-1}) + \epsilon_t$
- linear AR-1: $\ln(C_{i,t}) = \alpha + \beta \ln(C_{j,t-1}) + \epsilon_t$
- linear AR-2: $\ln(C_{i,t}) = \alpha + \beta_1 \ln(C_{j,t-1}) + \beta_2 \ln(C_{k,t-2}) + \epsilon_t$
- DLM AR-1: $\ln(C_{i,t}) = \alpha_t + \beta_t \ln(C_{j,t-1}) + \epsilon_t$
- GAM AR-1: $\ln(C_{i,t}) = \alpha + s(\ln(C_{j,t-1})) + \epsilon_t$
- GAM AR-2: $\ln(C_{i,t}) = \alpha + s_1(\ln(C_{j,t-1})) + s_2(\ln(C_{k,t-2})) + \epsilon_t$,

$\ln(C_{i,t})$, $\ln(C_{j,t-1})$, $\ln(C_{k,t-2})$ are the log catches. t, t-1, and t-2 denote current, prior year, and two years prior. i, j and k denote the season: July–September (denoted S for late-summer) or October–March (denoted W for winter) catch depending on the model.

We tested models with October–March (W_{t-1} and W_{t-2}), and July–September (S_{t-1} and S_{t-2}) catches 1 and 2 prior years as the explanatory catch variables (the $C_{j,t-1}$ and $C_{k,t-2}$). S_t was not used as a predictor for W_t because it is the immediately preceding quarter.

The catch models were fit to 1983–2015 catch data, the time period for which our SST, upwelling, and precipitation data were available for all years; we used the same years of catch data for all covariate tests. Akaike information criterion corrected for small sample size (AICc) and leave-one-out cross-validation (LOOCV) were applied to nested sets of models to evaluate model support. LOOCV involves model fitting with the omission of a data point, followed by prediction of that data point. The root mean-squared error (RMSE) and median absolute error (MdAE) are reported for the set of LOOCV prediction errors. After selection of the best model

TABLE 2 Best-performing GAM models for the July–September (S_t) and October–March (W_t) catches. M is the base model with only prior catch as covariates. To the base models, the environmental covariates are added. Nearshore SST is 0–80 km from the coast and regional SST is 0–160 km. The full set of nested covariate models with all tested environmental variables are given in Tables A1, A2 and Table S7

Model	Res. *df*	Adj. R^2	RMSE	AICc	LOOCV RMSE	LOOCV MdAE
July–Sept catch 1983–2015						
Null model:$\ln(S_t) = \ln(S_{t-1}) + \epsilon_t$	33		1.60	126.6	1.60	0.56
M0:$\ln(S_t) = \alpha + s(\ln(W_{t-1})) + \epsilon_t$	30	21.7	1.20	115.2	1.31	0.69
Covariate model: $\ln(S_t) = M0 + s(V)$						
V = Jun–Sep nearshore SST *t*	27.4	32.5	1.07	115.2	1.31	0.62[‡‡]
V = Jun–Jul precipitation over land *t*	28	29.9	1.10	115.3	1.33	0.62[‡‡]
V = 2.5-year ave. regional SST *t*	28.1	47	0.96	105.7[‡‡]	1.38	0.56[‡‡]
V = AMO ave. Jul–Jun *t*	27.5	47.5	0.94	106.6[‡‡]	1.22[‡]	0.56[‡‡]
October–March catch—simpler model 1983–2014						
Null model:$\ln(W_t) = \ln(W_{t-1}) + \epsilon_t$	32		1.00	92.9	1.00	0.26
M1:$\ln(W_t) = \alpha + s(\ln(W_{t-1})) + \epsilon_t$	29.1	45.9	0.82	87.7	0.96	0.32
Covariate model: $\ln(W_t) = M1 + s(V)$						
V = Jun–Jul precipitation over land *t*	26.9	59.6	0.69	82.1[‡‡]	0.91[‡]	0.25[‡‡‡]
V = 2.5-year ave. regional SST *t*	27.1	65.9	0.63	76.4[‡‡]	0.77[‡‡]	0.41
V = Sep–Nov DMI *t–1*	26	44.4	0.79	94.3	0.95	0.34
V = AMO ave. Jul–Jun *t*	26.6	63.8	0.64	79.4[‡‡]	0.81[‡‡]	0.38
October–March catch—more complex model 1983–2014						
M2:$\ln(W_t) = \alpha + s(\ln(W_{t-1})) + s(\ln(S_{t-2})) + \epsilon_t$	26.6	57.3	0.70	84.6	1.06	0.34
Covariate model: $\ln(W_t) = M2 + s(V)$						
V = Jun–Jul precipitation over land *t*	24.6	70.5	0.56	77.5[‡‡]	0.96[‡]	0.29[‡‡]
V = 2.5-year ave. regional SST *t*	24.8	69.5	0.57	78.1[‡‡]	0.82[‡‡‡]	0.35
V = Sep–Nov DMI *t–1*	23.8	69.1	0.56	81.1[‡]	0.87[‡‡]	0.34
V = AMO ave. Jul–Jun *t*	24.3	65.6	0.60	83.1	0.91[‡‡]	0.29[‡‡]

AICc, Akaike Information Criterion corrected for small sample size; LOOCV, Leave one out cross-validation; MdAE, median absolute error; RMSE, root mean square error. Res. df, residual degrees of freedom; Adj. R^2, adjusted R^2.

† and † † =AICc > 2 and >5 below base catch model (M). ‡, ‡ ‡, and ‡ ‡ ‡ =LOOCV RMSE and MdAE 5%, 10% and 20% below model M, respectively. **t** indicates the covariate from the current year while *t-1* indicates from the prior year. For covariates that are multiyear, t is the last calendar year (i.e., the 2014 multiyear average regional SST is January 2012 to June 2014). The equations with s() are GAM models where the covariates has a non-linear response (defined by a spline based smoothing function). The full set of nested tests for the base catch models (no environmental covariates) are given in the Supporting Information, Tables S1–S6.

using the 1983–2015 data, fitting was repeated with catch data from 1956–1982 to confirm the base catch model. An influential years test was performed by removing each year in the series sequentially and repeating the model selection analysis (Supporting Information: Validation of catch base models, Figures S1–S5).

2.4 | Covariate analysis

Once the base catch models were determined, the environmental covariates (Section 2.2) were studied. The covariate models were selected to test specific hypothesized drivers of catch variability based on how and when environmental variables are thought to affect oil sardine survival and recruitment and to affect availability to the fishery (summarized in Table 1 and Section 2.2). As with the catch models, support was evaluated using AICc and LOOCV with nested

sets of models. The full sets of nested models are shown in the appendices (Tables A1 and A2) and Supplement Table S7. Models with covariates (V) with linear and non-linear (GAM) effects were compared: $\ln(C_{i,t}) = M + \alpha + \beta V_t + \epsilon_t$ and $\ln(C_{i,t}) = M + \alpha + s(V_t) + \epsilon_t$, where M is the best catch model from the preliminary model fitting step described above. The smoothing term for the GAM models was fixed at an intermediate value (sp = 0.6). Note, in all cases, prior catch was the most important variable; that is, the environmental covariates were never more important than prior catch in terms of explaining variance.

Research has suggested that nutrient input from river discharge is necessary in order for upwelling to fuel high nearshore productivity (Shafeeque et al., 2019). To test this, models with a linear or non-linear upwelling-precipitation interaction were also tested: $\ln(C_{i,t}) = M + \alpha + \beta_1 V_{1,t} + \beta_2 V_{2,t} + \beta_3 V_{1,t} V_{2,t} + \epsilon_t$ and $\ln(C_{i,t}) = M + \alpha + s_1(V_{1,t}) + s_2(V_{2,t}) + ti(V_{1,t}, V_{2,t}) + \epsilon_t$, where *ti*( ) is

a tensor product interaction (non-linear interaction). Chlorophyll-a was not included in the main analyses since it is only available since September 1997. Instead, a separate analysis using 1997–2015 data was performed using chlorophyll-a alone as a covariate. Lastly, a DLM covariate model was used to explore models with changing effects of SST, AMO, and precipitation: $\ln\left(C_{i,t}\right) = M + \alpha_t + \beta_t V_t + \epsilon_t$.

All statistical analysis was completed in the R programming language (R Development Core Team, 2019) using the mcgv (Wood, 2011) and MARSS (Holmes et al., 2012) R packages.

3 | RESULTS

3.1 | Base catch model selection

For 1983–2015 July–September catches, models with the October–March catch in the prior year [$\ln(W_{t-1})$] were strongly supported over the naïve model and over models with the prior-year July–September catch [$\ln(S_{t-1})$], and models with catch two years prior (Tables S1 and S2). Including prior catch with a non-linear response improved model fit and reduced LOOCV RMSE (Table S2). Three models had almost identical AICc and LOOCV RMSE (maximum adjusted R^2 = 21.7): linear and non-linear models with $\ln(W_{t-1})$ only, and a non-linear model with $\ln(W_{t-1})$ and $\ln(W_{t-2})$. Similar model selection results were obtained for the October–March landings (Tables S4 and S5), but these models explained much more variance (maximum adjusted R^2 = 57.3). The best-supported model, based on AICc and F values, was the non-linear model with $\ln(W_{t-1})$ and $\ln(S_{t-2})$ (Table 2, S4 and S5). The simpler model with only $\ln(W_{t-1})$ had the second lowest AICc but lowest LOOCV RMSE values.

Repeating the model selection using 1956–1982 data yielded the same results for the July–September catch, with the non-linear model with $\ln(W_{t-1})$ having the lowest AICc and LOOCV RMSE values (Table S3). For the October–March catch, the results were very similar, but not identical. The non-linear model with $\ln(W_{t-1})$ had the lowest LOOCV RMSE and AICc values, while the models with $\ln(W_{t-1})$ and $\ln(S_{t-1})$ or $\ln(S_{t-2})$ had the second and third lowest AICs, although the difference from the AICc for the $\ln(W_{t-1})$ model was <3 (Table S6). The DLMs (time-varying effects) performed poorly for the July–September catch, with high AICc and LOOCV RMSE values. One DLM for the October–March catch showed mixed performance, with a higher AICc but lower LOOCV RMSE value. Overall, the model selection indicated that a catch model with a time-varying effect of prior catch did not improve either model fit or out-of-sample prediction, but inclusion of a non-linear effect was important.

We chose the non-linear model with $\ln(W_{t-1})$ as the base catch model for the July–September catch based on further diagnostic tests (Supporting Information: Validation of catch base models) and to minimize the loss of degrees of freedom from an additional covariate, $\ln(W_{t-2})$.

M0: $-\ln\left(S_t\right) = \alpha + s\left(\ln\left(W_{t-1}\right)\right) + \epsilon_t$ (adj. R^2 = 21.7)

Two non-linear base models were chosen for the October–March catch:

M1: $-\ln\left(W_t\right) = \alpha + s_1\left(\ln\left(W_{t-1}\right)\right) + s_2\left(\ln\left(S_{t-2}\right)\right) + \epsilon_t$ (adj. R^2 = 45.9)
M2: $-\ln\left(W_t\right) = \alpha + s\left(\ln\left(W_{t-1}\right)\right) + \epsilon_t$ (adj. R^2 = 57.3)

Both models were included as base models for the October–March catch as one had the best model fit while the other had better out-of-sample prediction. Both were supported based on the influential years analysis (Supporting Information; Figures S1–S5).

3.2 | Environmental covariate selection

The covariate analysis was able to rule out a number of the tested covariates. Specifically, we found no support for the use of April–May or June–July precipitation over the ocean, in the current or prior season or as a linear or non-linear effect, as an explanatory variable for the July–September or October–March catch (Tables A1, A2, and S7). We also found no support for the use of March–May (current or prior year) or October–December SST as an explanatory variable for the July–September or October–March catch (Tables A1, A2, and S7). In general, all the indices of upwelling in the current or prior year were either not or only weakly supported (based on AICc) and did not improve out-of-sample prediction (LOOCV RMSE or MdAE) (Tables A1, A2, and S7). The one exception was the July–September catch and the June–September nearshore SST upwelling index in the current year and Ekman Pumping in the prior year. These reduced the LOOCV MdAE prediction errors but did not reduce the LOOCV RMSE errors or AICc for the July–September catch (Table A1). The Ekman Mass Transport (EMT) upwelling index did not improve the model fit (AICc) or prediction errors (Table A1 and A2). Recent research (Shafeeque et al., 2019) suggests that there is an interaction between upwelling and precipitation, such that both anomalous precipitation over land and upwelling intensity during the summer monsoon is needed for strong chlorophyll-a blooms. Our tests using a variety of interaction models showed that while models with interactions increased the R^2, the increased parameter cost led to higher AICc and higher out-of-sample prediction errors (Table A8). Note, the July–September upwelling indices overlap with the July–September catch and thus would not be useful for forecasting July–September catch but were tested to understand the utility of the upwelling indices. We also found no support for using the ONI or PDO index to improve either the July–September or October–March catch predictions. The fall DMI in the prior year reduced AICc and LOOCV RMSE and MdAE but only for October–March catch with the more complex model (Table 2 and S7).

Only three covariates emerged as explanatory variables that both explained catch variance (lower AICc) and reduced out-of-sample predictions errors across models and across different time

periods: the June–July precipitation over land, the 2.5-year average regional SST, and the AMO index. The best models included non-linear response curves (Figure 6). For the July–September catch, the best models had an adjusted R^2 of 29.9, 47, and 47.5 (precipitation, SST, and AMO, respectively) versus 21.7 for the model without the covariate (Tables 2 and A1), and for the October–March catch, the adjusted R^2 was 59.6, 65.9 and 63.8 (precipitation, SST and AMO) versus 45.9 using the simpler base model without covariates and 70.5, 69.5 and 65.6 versus 57.3 with the more complex base model (Tables 2, A2, and S7). These covariates reduced the median out-of-sample prediction error (LOOCV MdAE) by up to 19% for the July–September catch and the root mean-squared and median out-of-sample prediction errors (LOOCV RMSE and MdAE) by up to 22% for the October–March catch relative to the base model without environmental covariates (Tables 2, A1, A2, and S7). Figure 7 illustrates the reduction in prediction errors using the 2.5-year average regional SST as an example (the other covariates are shown in Figures A1 and A2).

Our examination of the chlorophyll-a covariate was limited, as the simplest model including the chlorophyll-a concentration required five degrees of freedom, and catch size varied little in the period for which we had chlorophyll-a data. The fitting of second-degree polynomial models to the average log chlorophyll-a concentrations in July–September and October–December of the current and prior years yielded no significant result for the July–September catch, but we found a significant effect of the prior-year October–December chlorophyll-a concentration on the October–March catch (Tables A1, A2 and S7).

We identified four outlier years in which October–March oil sardine landings were much lower than predicted based on prior catches: 1986, 1991, 1994, and 2013 (Figure 7c). In the figure, the y-axis is the predicted catch in a LOOCV analysis thus is the "left-out" year. The model with 2.5-year average regional SST predicted the collapses in 1986 and 1991; the predicted catch sizes with this covariate in the model were much closer to the observed catches (Figure 7d). The 2.5-year average regional SST did not explain the 1994 collapse, the largest during the study period, or the 2013 collapse. The same pattern was seen for the July–September catch, with the exception that this catch was not unusually low in 1991 (Figure 7a). The 2.5-year average regional SST reduced the prediction errors for this catch in 1986 but did not (appreciably) reduce it for 1994 or 2013 (Figure 7b). In fact, no covariate tested in this study explained the 1994 fishery collapse (Figures A1 and A2); the prediction error for this year was very high regardless of any covariate that was included in the model.

3.3 | Dynamic linear modeling with SST, AMO and precipitation

The ICOADS SST data set does not capture the nearshore SST as accurately as AVHRR, and thus was not used for our main analyses. Nonetheless the ICOADS regional SST (as opposed to nearshore) is highly correlated with the AVHRR regional SST data (Supporting

Information; Figure S7), and the ICOADS SST data extend almost to the start of the catch time series (to 1960). The precipitation data and AMO index also extend to 1960. Using the dynamic linear model for the October–March catch, we examined whether the explanatory power (as measured by model residual errors, i.e., model fit) of these three covariates changed over time. Time-varying covariate models were fit to the residuals of the simpler base October–March catch model; the results were very similar with the more complex October–March catch model thus results using only one of the October–March base models are shown. The covariates were z-scored (mean removed and variance standardized to 1) and included as third-order polynomials to allow a non-linear response. The models took the form $r_t = \beta_{1,t}V_t + \beta_{2,t}V_t^2 + \beta_{3,t}V_t^3 + \epsilon_t$ where r is the catch residual and V is the covariate. The β was allowed to evolve as an autoregressive process, $\beta_t = \beta_{t-1} + e_t$, with $e_t \sim N(0, \sigma)$. The σ was chosen such that the model complexity (time-variation) did not increase out-sample-prediction error over the base catch model (with no environmental covariates).

The explanatory power of the covariates, even when allowed to be time-varying and thus flexible enough to fit temporally local conditions, changed over time. Up to 1990, the land precipitation did not increase model fit but did afterward. The 2.5-year average regional SST and AMO index improved the model fit over the entire time series (meaning the covariate RMSE line was below that of the model with no covariates), but especially so from the mid-1980s to late-1990 s (Figure 8).

4 | DISCUSSION

Our results indicate that successful modeling of Indian oil sardine catch depends on the catch season of interest (monsoon versus post-monsoon) and selection of the environmental covariate to use in the model. All the covariates we tested were tied to environmental conditions known to impact key life stages of the oil sardine. However only two regional covariates, the multiyear average regional SST and the monsoon rainfall over land, and one ocean climate index, the Atlantic Multidecadal Oscillation index, improved both model fit and out-of-sample prediction.

4.1 | Monsoon versus post-monsoon model performance

The July–September catch, which overlaps with the summer monsoon and a seasonal fishery closure, is difficult to model. The best July–September models with only prior catch as a covariate explained less than 22% of the variation while the best model with environmental covariates explained only 47% of the variation and had median out-of-sample prediction errors of +/−65% (of raw, not log-transformed, catch). We found only one covariate that improved the root mean-squared out-of-sample prediction error for the July–September catch (the AMO index), though a number improved median out-of-sample prediction
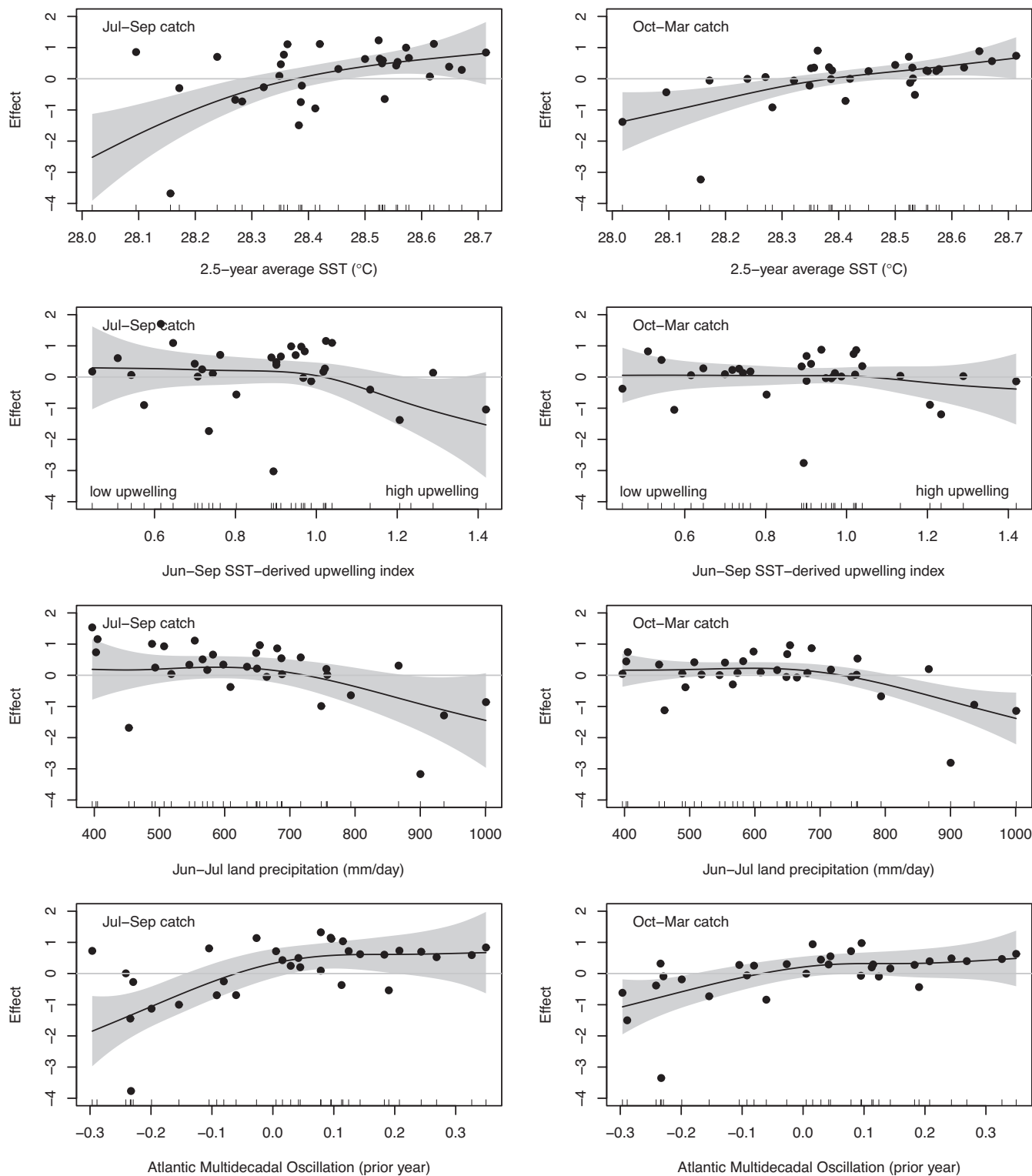
FIGURE 6 Effect sizes for the 2.5-year average regional sea surface temperature (SST; within 2° of the Kerala coast), current-season upwelling intensity (average June–September SST nearshore-offshore upwelling index off Kochi, Kerala), current season June–July precipitation over land and the Atlantic Multidecadal Oscillation (AMO) index in the prior year on July–September and October–March catches. As the upwelling index reflects the difference between offshore and nearshore SST, positive values indicate that coastal surface waters are colder than offshore waters. The more positive the difference, the stronger the upwelling intensity

error. In contrast, variation in the post-monsoon catch (October–March) was much better explained. The simpler model with only prior catch as a covariate explained 45.9% of the variation and the model with the best covariate, explained 65.9%. The best environmental covariate reduced the out-of-sample prediction errors (RMSE and MdAE) by ca. 20% and explained two of the four recent catch collapses.
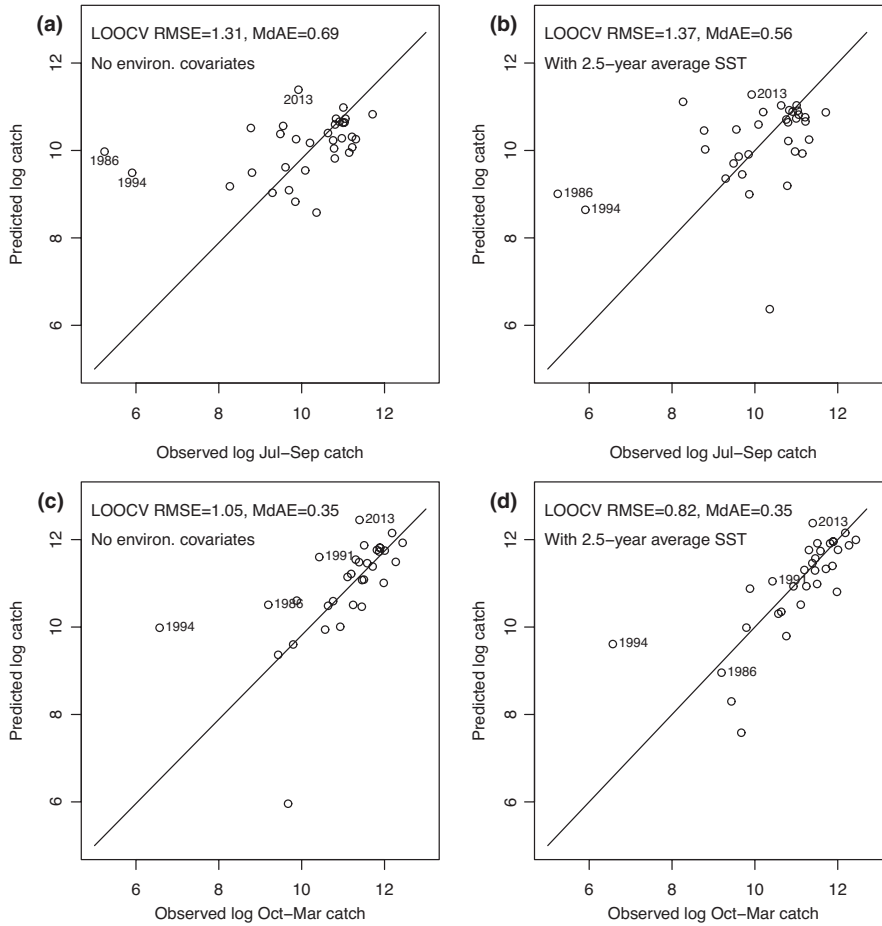
FIGURE 7 Predicted versus observed catches obtained with models with and without the 2.5-year average sea surface temperature (SST) included as a non-linear covariate. The lines indicate a perfect prediction where observed catch equals the predicted catch. The value to be predicted was left out in the model fitting. Values above the line are cases where the prediction was too high and values below the line are cases where the prediction was too low. (a) July–September catch, modeled with only the prior-season October–March catch as a covariate. (b) July–September catch, modeled with the prior-season October–March catch and 2.5-year average SST as covariates. (c) October–March catch, modeled with the prior-season October–March catch only. (d) October–March, modeled as in panel c with the addition of the 2.5-year average SST. LOOCV RMSE =leave-one-out root mean-squared prediction error. See Figures A1 and A2 for the same plots with other environmental covariates
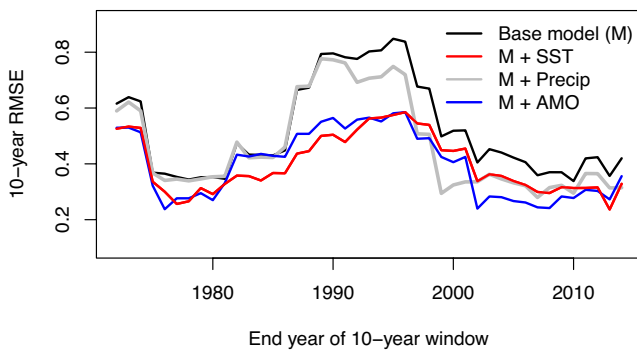

FIGURE 8 Model fit over 10-year windows for dynamic linear models of October–March catch 1960–2015 using the 2.5-year average SST from the ICOADS data set, June–July precipitation over land (from land gages), and Atlantic Multidecadal Oscillation index as covariates. These models allowed the covariate model to evolve over time. The models were fit to the residuals of the simpler base model (with only prior October–March catch as a covariate) with the 1994 residual removed. The covariates were z-scored (mean removed and standardized to variance of 1) and included as a third-order polynomial to allow a non-linear effect. The plot shows the RMSE of the model residuals computed on a 10-year sliding window

This result cautions against modeling all quarters of oil sardine catch together (as one yearly catch). The July–September catch is difficult to model, as it exhibits high variability that is poorly explained by past catches or environmental factors. The reasons for this are likely a combination of variable spawning timing which affects the timing of movement of adults into the nearshore where they are exposed to the fishery, the summer monsoon which affects fishing operations, and the fishery closure during part of this period. In contrast, the October–March catch, which comprises 60–80% of the catch from July to June, is much better explained, and its forecasts have smaller predictive errors. Forecasting all quarters together as a yearly catch means that the high variability in the July–September catch will hide the predictability of the subsequent October–March catch.

4.2 | Sea surface temperature

The SST in October–December, the period of larval and early juvenile development, may affect survival and growth in multiple ways and thus correlate with biomass in future years. In some years, extreme heat events occur in March–May during the period of egg maturation which may affect spawning and thus the current year and future biomass. However, we found no correlation of these seasonal SST

covariates with the July–September or October–March catch in the current or future years.

Instead, we found that the regional SST averaged over the prior 2.5 years (January t-2 to June t), corresponding to the life span of an oil sardine, emerged as a consistently informative SST covariate. The multiyear average regional SST explained variability in the oil sardine landings and improved out-of-sample catch prediction. Studies conducted in the California Current System have also found that the multiyear average SST explains year-to-year variability in Pacific sardine recruitment (Checkley et al., 2009, 2017; Jacobson & MacCall, 1995; Lindegren & Checkley, 2013). This covariate has also been found to correlate with southern African sardine recruitment (Boyer et al., 2001). McClatchie, Goericke, Auad, and Hill (2010) found no relationship between SST and Pacific sardine recruitment; however, they examined this relationship linearly; in the present study, as in the other cited studies, allowance of non-linearity in the SST effect was important. Both Jacobson and MacCall (1995) and Lindegren and Checkley (2013) found a step-like response function for temperature: below a threshold value the effect of temperature was linear (and positive) and above the threshold, the effect was flat (no longer increased). In the linear portion of the effect curve, the point where the effect curve crosses from negative to positive represents an important biological threshold. Our analysis found a similar effect curve with a negative effect when the 2.5-year average regional SST was below 28.37°C and positive above and with the positive effect leveling off above 28.5°C.

The AMO index (July t-1 to June t average) is highly correlated with the 2.5-year average regional SST covariate used in our analyses (Pearson correlation $\rho = 0.70$ 1983–2016), unlike the other ocean climate indices: ONI $\rho = 0.16$, PDO index $\rho = -0.04$ and DMI $\rho = 0.37$ (Supporting Information; Figure S8). Thus, not surprisingly, the AMO index also emerged as a consistently informative covariate and provided reductions in out-of-sample prediction error similar to the multiyear average SST. None of the other ocean climate indices were informative, except the DMI but only in the most complex October–March catch model. Teleconnection between the AMO and the Indian Ocean has been shown in a number of papers (reviewed in Hu, Hu & Hu, 2018; Zhang et al., 2019). In particular, there appears to be a relationship between the intensity of the Indian summer monsoon and the AMO (Lu et al., 2006; Zhang & Delworth, 2006). The correlation between oil sardine landings and the AMO index that we (and Hamza et al., 2020) found is likely a reflection of this large-scale teleconnection that manifests, in part, as correlation between regional SST and the AMO index.

4.3 | Precipitation

Since early studies of oil sardines, precipitation during the summer monsoon has been studied as a variable to explain catch fluctuations (Antony Raja, 1969, 1974; Murty & Edelman, 1966; Srinath, 1998). While correlations have been found, the identified correlations between precipitation and oil sardine landings have been positive in

some studies and negative in others (Madhupratap et al., 1994) and varied depending on the time period studied. In general, the correlation was assumed to be positive as rainfall is correlated with monsoon intensity which is in turn correlated with upwelling and productivity. But heavy monsoon rain also has negative effects. During heavy rainfall, nutrient and sediments flow into the nearshore region from rivers, which leads to short-term eutrophication and anoxia in coastal waters (Chauhan et al., 2011).

In our study, we compared rainfall over the ocean (using remote-sensing data) and over the land (using land-gauge data). Though correlated, these are not identical. We found no correlation between rainfall over the ocean and catch in any combination of our statistical tests. Oceanic rainfall was uniformly disinformative—increasing both AICc and out-of-sample prediction errors—across all combinations of models tested. In contrast, the June–July precipitation over land in the current season was strongly informative and was the only covariate besides the multiyear average regional SST and AMO index that improved model fit and out-of-sample prediction. The effect of precipitation was non-linear; close to zero for low to moderate rainfall levels and then negative at high precipitation. This suggests that the negative effect of high rainfall was the dominant impact. The effects were only seen on the current-year catch and thus may reflect a temporary movement of fish offshore (away from the fishery) to avoid anoxia rather than a lower cohort strength that would persist into the next season.

4.4 | Upwelling

Despite the strong connections of upwelling with productivity which positively impacts sardine recruitment, growth, and survival, none of the upwelling indices examined in this study (SST-nearshore-offshore differential, Ekman Mass Transport, and Ekman Pumping) explained year-to-year variation in current-year or prior-year landings or improved out-of-sample forecasts. When we did find a (weak) relationship with upwelling intensity and catch, the effect was for the current year only and was negative, rather than positive. The negative effect emerged at extremely high upwelling. This negative effect is not surprising. Extremely high upwelling transports larval sardines offshore and brings to the surface poorly oxygenated water which sardines avoid (Gupta et al., 2016).

Our tests looked at whether upwelling intensity explained variation and future catch beyond what could be explained using a catch model with only prior catch as the covariate. It may be that upwelling affects the future abundance in a way that is already captured by using prior catch. Conversely, it may be that strong upwelling by itself is not sufficient for productivity. Shafeeque et al., (2019) looked at the correlation between summer upwelling strength and precipitation and chlorophyll-a bloom intensity. They found that chlorophyll-a bloom anomalies were associated with years with both upwelling and precipitation anomalies, suggesting an interaction between these two environmental variables. While we found that models with an upwelling and

precipitation interaction did have higher R^2 relative to an upwelling-only or precipitation-only model, they had higher, sometimes considerably higher, out-of-sample prediction errors than the base catch model with no covariates or the base catch model with only precipitation. This highlights one of the dilemmas of forecasting: increased complexity in a model often brings a high prediction cost.

The monthly average upwelling metrics we used are those used in many other studies of upwelling and nearshore productivity in this region. In most coastal upwelling systems, local wind-stress forces are the most important driver of upwelling; however, the southwest coast of India is unique in that remote-forcing and local currents and gyres play an unusually important role in driving the seasonal upwelling intensity (BR, 2010; BR et al., 2008; Rao et al., 2008; Shah et al., 2019). Our nearshore-offshore SST differential index should have captured upwelling intensity due to either wind stress or remote forcing, and we expected that it would perform better than the wind-based metrics. However, it was equally uninformative as a covariate. It may be that other aspects of upwelling besides average nearshore intensity, such as the timing of its initiation (e.g., Barth et al., 2007), its spatial extent along the coast or some metric of daily extreme events are necessary to capture the conditions relevant to oil sardine landings. We did find support for a more direct measure of productivity and food availability: the nearshore surface chlorophyll-a concentration. Chlorophyll-a concentration in fall, the period of peak juvenile somatic growth, explained the October–March catch in the next year, reducing out-of-sample prediction errors by 10% to 20%. With chlorophyll-a data only available after 1997, the power of our tests was limited, but this suggests that fall chlorophyll-a concentration, after the summer peak chlorophyll-a blooms, may prove useful for improving forecasts.

4.5 | Oil sardine collapses

There were four years when October–March oil sardine landings were much lower than expected based on prior catches: 1986, 1991, 1994, and 2013. The 2.5-year average regional SST was able to explain the collapses in 1986 and 1991. The largest collapse was in 1994, when the catch was much lower than expected even taking into account the prior-year declines. The most recent collapse, in our data set, was 2013. The 2.5-year average regional SST did not successfully predict the 1994 or 2013 collapses; although the prediction error was reduced for both years, it was still large. The same pattern was seen for the July–September catch, with the exception that 1991 was not unusually low. The 2.5-year average regional SST reduced the prediction error for 1986 but did not (appreciably) for 1994 nor 2013. In fact, none of the covariates we tested explained the lower than expected 1994 catch; while only the precipitation over land in June–July explained the 2013 collapse (but not 1994, 1991, nor 1986). The 1994 collapse was correlated with severe nearshore anoxia (Kripa et al., 2015). Since none of the environmental factors we studied captured the 1994 decline, it suggests that metrics that more directly measure nearshore anoxia may be necessary.

5 | CONCLUSIONS

Our study emphasizes a number of key points for developing models for the purpose of landings forecasting. First, improvements in catch forecasts beyond what is possible using prior catch (a null autoregressive catch model) may be elusive. All the environmental covariates that we tested are closely tied to factors that affect critical months of spawning, growth, survival, and movement of sardines into the nearshore (where they are exposed to the fishery). Yet almost none of these explained catch variability, beyond what could be explained using a simple autoregressive catch model. Second, non-linear effects are common and important to consider. Third, covariate effects can change over time. Fisheries exist within complex multi-species ecological systems and species and their life histories evolve. Forecast models will need to guard against covariate effects that change over time and lead to an erosion of forecast performance. Lastly, model complexity comes at a price particularly when the goal is prediction. Inclusion of out-of-sample prediction metrics is crucial as these can give a very different picture compared with metrics for model fit alone. Covariates that are supported by model fit, even using model selection metrics that penalize extra complexity, may still be uninformative or even disinformative for out-of-sample prediction.

Despite all this, we found that there were environmental covariates that did appreciably improve landings prediction. In particular, the multiyear average sea surface temperature has now emerged as an informative covariate across multiple studies on sardine species, and interestingly, the Atlantic Multidecadal Oscillation index—recently shown to be correlated to oil sardines landings by Hamza et al., (2020)—was also an informative covariate in our analysis. This suggests that the Indian oil sardine is affected by global-scale processes, in particular the teleconnection between the AMO and Indian Ocean processes (reviewed in Hu, Hu & Hu, 2018; Zhang et al., 2019). We see a number of fruitful directions to explore to further improve short-term forecasts. The first is incorporation of direct leading indicators of catch. We did not show models with catch in the prior quarter as a predictor; surveys take time to process and report and thus data for the immediately prior quarter would not be available. Had we included the prior quarter catch, the fits and predictions would be much better. However, models could use preliminary catch numbers from the beginning of the prior quarter from sentinel landing centers or gear types. This would be feasible without a new data collection scheme and would certainly improve the short-term forecasts for the next quarter. A longer-term approach would be incorporation of recruitment information from egg or larval density surveys. Such surveys have been conducted on the U.S. West coast since the 1940 s by the California Cooperative Oceanic Fisheries Investigations (CalCOFI) Program (Gallo et al., 2019), and these data have been successfully used to improve abundance estimation and management of the Pacific sardine (McClatchie, 2014). Leading abundance indicators, such as from preliminary catch data or larval surveys, are likely to be especially important if climate changes alter past relationships of catch with the environmental covariates.

The temperature of the Western Indian Ocean has been increasing over the last century at a greater rate than in any other tropical ocean (Roxy et al., 2014), and warming has been most extreme during the summer monsoon months. These changes are affecting the oil sardine distribution, with significant landings now occurring north of Goa (Vivekanandan et al., 2009). Continued warming is expected to affect the productivity of the region via multiple pathways, including changes in salinity, oxygen concentration, currents, wind patterns, ocean stratification, and upwelling spatial patterns, phenology, and intensity (Moustahfid, Marsac, & Grangopadhyay, 2018). The incorporation of environmental covariates into landings forecasts has the potential to improve fishery management for small pelagic species, such as oil sardines, in the face of a changing ocean environment (Haltuch et al., 2019; Tommasi et al., 2016). However, careful performance testing of the environmental covariates will be needed and expectations as to how much environmental covariates can improve forecasts should be tempered, especially if there are multi-month lags in the landings data available to include in the forecast or if new sources of abundance indicators, such as recruitment surveys, remain unavailable.

CONFLICT OF INTEREST

The authors have no conflicts of interest to declare.

AUTHOR CONTRIBUTIONS

All authors were involved in the conceptualization and writing—review and editing. Individual authors had these additional roles. Elizabeth Holmes: Data curation, methodology, formal analysis, software, and writing—original draft. Smitha BR: Writing—original draft. Kumar Nimit: Data curation and writing—original draft. Sourav Maity: Visualization. David Checkley and Mark Wells: Methodology, writing—revisions and review. Vera Trainer: Funding acquisition and project supervision.

DATA AVAILABILITY STATEMENT

The raw data that supports the findings of this study are available in the data table in the supplementary material of this article. The data were derived from the following resources available in the public domain. SST, chlorophyll-a concentration, and ocean currents: NOAA ERDDAP data server https://coastwatch.pfeg.noaa.gov/erddap. Ocean winds from the ERA5 Global Reanalysis: Asia-Pacific Data Research Center ERDDAP data server http://apdrc.soest.hawaii.edu/erddap. Ocean precipitation: NOAA/NCEI Global Precipitation Climatology Project https://www.ncei.noaa.gov. Land precipitation: Open Government Data Platform India https://data.gov.in. ONI: U.S. National Weather Service Climate Prediction Center https://www.cpc.ncep.noaa.gov. DMI: Japan Agency for Marine-Earth Science and Technology http://www.jamstec.go.jp. PDO and AMO: U.S. NOAA Physical Sciences Laboratory https://psl.noaa.gov/. Landings data: Reports and databases published by the Central Marine Fisheries Research Institute http://www.cmfri.org.in.

ORCID

Elizabeth Eli Holmes https://orcid.org/0000-0001-9128-8393
Smitha BR https://orcid.org/0000-0003-3470-9272
Kumar Nimit https://orcid.org/0000-0002-3815-5919
Sourav Maity https://orcid.org/0000-0003-2337-5457
David M. Checkley https://orcid.org/0000-0003-1885-252X
Mark L. Wells https://orcid.org/0000-0003-2028-9553
Vera L. Trainer https://orcid.org/0000-0001-6553-0369

REFERENCES

Alheit, J., Gröger, J., Licandro, P., McQuinn, I. H., Pohlmann, T., & Tsikliras, A. C. (2019). What happened in the mid-1990s? The coupled ocean-atmosphere processes behind climate-induced ecosystem changes in the Northeast Atlantic and the Mediterranean. *Deep Sea Research Part II: Topical Studies in Oceanography.*, *159*, 130–142. https://doi.org/10.1016/j.dsr2.2018.11.011

Alheit, J., & Hagen, E. (1997). Long-term climate forcing of European herring and sardine populations. *Fisheries Oceanography*, *6*(2), 130–139. https://doi.org/10.1046/j.1365-2419.1997.00035.x

Alheit, J., Pohlmann, T., Casini, M., Greve, W., Hinrichs, R., Mathis, M., O'Driscoll, K., Vorberg, R., & Wagner, C. (2012). Climate variability drives anchovies and sardines into the North and Baltic Seas. *Progress in Oceanography, 96*(1), 128–139. https://doi.org/10.1016/j.pocean.2011.11.015

Annigeri, G. G. (1969). Fishery and biology of the oil sardine at Karwar. *Indian Journal of Fisheries*, *16*(1/2), 35–50.

Antony Raja, B. T. (1964). Some aspects of spawning biology of Indian oil sardine *Sardinella longiceps* Valenciennes. *Indian Journal of Fisheries*, *11*(1), 45–120.

Antony Raja, B. T. (1969). Indian oil sardine. *CMFRI Bulletin*, *16*, 1–142.

Antony Raja, B. T. (1970). Estimation of age and growth of the Indian oil sardine, *Sardinella longiceps* Val. *Indian Journal of Fisheries*, *17*(1/2), 26–42.

Antony Raja, B. T. (1974). Possible explanation for the fluctuation in abundance of the Indian oil sardine, *Sardinella longiceps* Valenciennes. *Proceedings of the Indo-Pacific Fisheries Council*, *15*(3), 241–252.

Bakun, A., Roy, C., & Lluch-Cota, S. (2008). Coastal upwelling and other processes regulating ecosystem productivity and fish production in the western Indian Ocean. In K. Sherman, E. N. Okemwa, & M. J. Ntiba (Eds.), *Large marine ecosystems of the Indian Ocean: Assessment, sustainability and management* (pp. 103–141). Blackwell.

Barth, J. A., Menge, B. A., Lubchenco, J., Chan, F., Bane, J. M., Kirincich, A. R., McManus, M. A., Nielsen, K. J., Pierce, S. D., & Washburn, L. (2007). Delayed upwelling alters nearshore coastal ocean ecosystems in the northern California Current. *Proceedings of the National Academy of Sciences*, *104*(10), 3719–3724. https://doi.org/10.1073/pnas.0700462104

Bensam, P. (1964). Growth variations in the Indian oil sardine, *Sardinella longiceps* Valenciennes. *Indian Journal of Fisheries*, *11A*(2), 699–708.

Boyer, D. C., Boyer, H. J., Fossen, I., & Kreiner, A. (2001). Changes in abundance of the northern Benguela sardine stock during the decade 1990 to 2000 with comments on the relative importance of fishing and the environment. *South African Journal of Marine Science*, *23*(1), 67–84. https://doi.org/10.2989/025776101784528854

BR, S.(2010). *Coastal upwelling of the south eastern Arabian Sea — an integrated approach*. Kerala, India: PhD Thesis. Physical Oceanography. Cochin University of Science and Technology.

BR, S., Sanjeevan, V. N., Vimalkumar, K. G., & Revichandran, C. (2008). On the upwelling of the southern tip and along the west coast of India. *Journal of Coastal Research*, *24*(sp3), 95–102. https://doi.org/10.2112/06-0779.1

Chauhan, O. S., Raghavan, B. R., Singh, K., Rajawat, A. S., Ajai, Kader, U. S. A., & Nayak, S. (2011). Influence of orographically enhanced SW monsoon flux on coastal processes along the SE Arabian Sea. *Journal of Geophysical Research. Oceans*, *116*(12), C12037. https://doi.org/10.1029/2011JC007454

Checkley, D. M. Jr, Alheit, J., Oozeki, Y., & Roy, C. (2009). *Climate change and small pelagic fish*. Cambridge University Press. https://doi.org/10.1017/CBO9780511596681

Checkley, D. M. Jr, Asch, R. G., & Rykaczewski, R. R. (2017). Climate, anchovy, and sardine. *Annual Review of Marine Science*, *9*, 469–493. https://doi.org/10.1146/annurev-marine-122414-033819

Cohen, Y., & Stone, N. (1987). Multivariate time series analysis of the Canadian fisheries system in Lake Superior. *Canadian Journal of Fisheries and Aquatic Sciences*, *44*(S2), 171–181. https://doi.org/10.1139/f87-321

Currie, J., Lengaigne, M., Vialard, J., Kaplan, D. M., Aumont, O., Naqvi, S. W. A., & Maury, O. (2013). Indian ocean dipole and El Niño/Southern Oscillation impacts on regional chlorophyll anomalies in the Indian Ocean. *Biogeosciences*, *10*(10), 6677–6698. https://doi.org/10.5194/bg-10-6677-2013

Cury, P., Bakun, A., Crawford, R. J. M., Jarre, A., Quinones, R. A., Shannon, L. J., & Verheye, H. M. (2000). Small pelagics in upwelling systems: Patterns of interaction and structural changes in "wasp-waist" ecosystems. *ICES Journal of Marine Science*, *57*(3), 603–618. https://doi.org/10.1006/jmsc.2000.0712

Das, P. H. D., & Edwin, L. (2018). Temporal changes in the ring seine fishery of Kerala, India. *Indian Journal of Fisheries*, *65*(1), 47–54. https://doi.org/10.21077/ijf.2018.65.1.69105-08

Farmer, N. A., & Froeschke, J. T. (2015). Forecasting for recreational fisheries management: What's the catch? *North American Journal of Fisheries Management*, *35*(4), 720–735. https://doi.org/10.1080/02755947.2015.1044628

Gallo, N. D., Drenkard, E., Thompson, A. R., Weber, E. D., Wilson-Vandenberg, D., McClatchie, S., Koslow, J. A., & Semmens, B. X. (2019). Bridging from monitoring to solutions-based thinking: lessons from CalCOFI for understanding and adapting to marine climate change impacts. *Frontiers in Marine. Science*, *6*, Article 695. https://doi.org/10.3389/fmars.2019.00695

Garza-Gil, M. D., Varela-Lafuente, M., Caballero-Míguez, G., & Torralba-Cano, J. (2015). A study on economic impact on the European sardine fishery due to continued global warming. In B. R. Singh (Ed.), *Global warming: Causes, impacts and remedies* (pp. 115–136). https://doi.org/10.5772/58877

Georgakarakos, S., Doutsoubas, D., & Valavanis, V. (2006). Time series analysis and forecasting techniques applied on loliginid and ommastrephid landings in Greek waters. *Fisheries Research*, *78*(1), 55–71. https://doi.org/10.1016/j.fishres.2005.12.003

George, G., Meenakumari, B., Raman, M., Kumar, S., Vethamony, P., Babu, M. T., & Verlecar, X. (2012). Remotely sensed chlorophyll: A putative trophic link for explaining variability in Indian oil sardine stocks. *Journal of Coastal Research*, *28*(1A), 105–113. https://doi.org/10.2112/JCOASTRES-D-10-00070.1

Gupta, G. V. M., Sudheesh, V., Sudharma, K. V., Saravanane, N., Dhanya, V., Dhanya, K. R., Lakshmi, G., Sudhakar, M., & Naqvi, S. W. A. (2016). Evolution to decay of upwelling and associated biogeochemistry over the southeastern Arabian Sea shelf. *Journal of Geophysical Research: Biogeosciences*, *121*(1), 159–175. https://doi.org/10.1002/2015JG003163

Habeebrehman, H., Prabhakaran, M. P., Jacob, J., Sabu, P., Jayalakshmi, K. J., Achuthankutty, C. T., & Revichandran, C. (2008). Variability in biological responses influenced by upwelling events in the eastern Arabian Sea. *Journal of Marine Systems*, *74*(1–2), 545–560. https://doi.org/10.1016/j.jmarsys.2008.04.002

Haltuch, M. A., Brooks, E. N., Brodziak, J., Devine, J. A., Johnson, K. F., Klibansky, N., Nash, R., Payne, M. R., Shertzer, K. W., Subbey, S., & Wells, B. K. (2019). Unraveling the recruitment problem: A review of environmentally-informed forecasting and management strategy evaluation. *Fisheries Research*, *217*, 198–216. https://doi.org/10.1016/j.fishres.2018.12.016

Hamza, F., Valsala, V., Mallissery, A., & George, G. (2020). Climate impacts on the landings of Indian oil sardine over the south-eastern Arabian Sea. *Fish and Fisheries*, *22*(1), 175–193. https://doi.org/10.1111/faf.12513

Hanson, P. J., Vaughan, D. S., & Narayan, S. (2006). Forecasting annual harvests of Atlantic and Gulf menhaden. *North American Journal of Fisheries Management*, *26*(3), 753–764. https://doi.org/10.1577/M04-096.1

Holmes, E. E., Ward, E. J., & Wills, K. (2012). MARSS: Multivariate autoregressive state-space models for analyzing time-series data. *The R Journal*, *4*(1), 11–19. https://doi.org/10.32614/RJ-2012-002

Hornell, J. (1910). Report on the results of a fishery cruise along the Malabar coast and to the Laccadive Islands in 1908. *Madras Fishery Bulletin*, *4*(4), 76–126.

Hornell, J., & Nayudu, M. R. (1924). A contribution to the life history of the Indian sardine with notes on the plankton of the Malabar coast. *Madras Fishery Bulletin*, *17*(5), 129–197.

Hu, Z., Hu, A., & Hu, Y. (2018). Contributions of interdecadal Pacific oscillation and Atlantic multidecadal oscillation to global ocean heat content distribution. *Journal of Climate*, *31*(3), 1227–1244. https://doi.org/10.1175/JCLI-D-17-0204.1

Jacobson, L. D., & MacCall, A. D. (1995). Stock-recruitment models for Pacific sardine (*Sardinops sagax*). *Canadian Journal of Fisheries and Aquatic Sciences*, *52*(3), 566–577. https://doi.org/10.1139/f95-057

Jayaprakash, A. A. (2002). Long term trends in rainfall, sea level and solar periodicity: A case study for forecast of Malabar sole and oil sardine fishery. *Journal of the Marine Biological Association of India*, *44*(1/2), 163–175.

Jayaprakash, A. A., & Pillai, N. G. K. (2000). The Indian oil sardine. In V. N. Pillai, & N. G. Menon (Eds.), *Marine fisheries research and management* (pp. 259–281). Central Marine Fisheries Research Institute.

Kripa, V., Mohamed, K. S., Koya, K. P. S., Jeyabaskaran, R., Prema, D., Padua, S., Kuriakose, S., Anilkumar, P. S., Nair, P. G., Ambrose, T. V., Dhanya, A. M., Abhilash, K. S., Bose, J., Divya, N. D., Shara, A. S., & Vishnu, P. G. (2018). Overfishing and climate drives changes in

biology and recruitment of the Indian oil sardine *Sardinella longiceps* in southeastern Arabian Sea. *Frontiers in Marine Science*, 5, Article 443. https://doi.org/10.3389/fmars.2018.00443

Kripa, V., Prema, D., Jeyabaskaran, R., Khambadkar, L. R., Nandakumar, A., Anilkumar, P. S. et al (2015). Inter-annual variations of selected oceanographic parameters and its relation to fishery of small pelagics off Kochi, southwest coast of India. *Journal of the Marine Biological Association of India*, 57, 52–57.

Krishnakumar, P. K., Mohamed, K. S., Asokan, P. K., Sathianandan, T. V., Zacharia, P. U., Abdurahiman, K. P., & Durgekar, N. R. (2008). How environmental parameters influenced fluctuations in oil sardine and mackerel fishery during 1926–2005 along the south-west coast of India? *Marine Fisheries Information Service, Technical and Extension Series*, 198, 1–5.

Lawer, E. A. (2016). Empirical modeling of annual fishery landings. *Natural Resources*, 7(3), 193–204. https://doi.org/10.4236/nr.2016.74018

Lindegren, M., & Checkley, D. M. Jr (2013). Temperature dependence of Pacific sardine (*Sardinops sagax*) recruitment in the California Current Ecosystem revisited and revised. *Canadian Journal of Fisheries and Aquatic Sciences*, 70(2), 245–252. https://doi.org/10.1139/cjfas-2012-0211

Lindegren, M., Checkley, D. M. Jr, Rouyer, T., MacCall, A. D., & Stenseth, N. C. (2013). Climate, fishing, and fluctuations of sardine and anchovy in the California Current. *Proceedings of the National Academy of Sciences*, 110(33), 13672–13677. https://doi.org/10.1073/pnas.1305733110

Lloret, J., Lleonart, J., & Sole, I. (2000). Time series modelling of landings in Northwest Mediterranean Sea. *ICES Journal of Marine Science*, 57(1), 171–184. https://doi.org/10.1006/jmsc.2000.0570

Longhurst, A. R., & Wooster, W. S. (1990). Abundance of oil sardine (*Sardinella longiceps*) and upwelling on the southwest coast of India. *Canadian Journal of Fisheries and Aquatic Sciences*, 47(12), 2407–2419. https://doi.org/10.1139/f90-268

Lu, R., Dong, B., & Ding, H. (2006). Impact of the Atlantic Multidecadal Oscillation on the Asian summer monsoon. *Geophysical Research Letters*, 33(24), L24701. https://doi.org/10.1029/2006GL027655

Madhupratap, M., Gopalakrishnan, T. C., Haridas, P., & Nair, K. K. C. (2001). Mesozooplankton biomass, composition and distribution in the Arabian Sea during the fall intermonsoon: Implications of oxygen gradients. *Deep Sea Research Part II: Topical Studies in Oceanography*, 48(6), 1345–1368. https://doi.org/10.1016/S0967-0645(00)00142-9

Madhupratap, M., Shetye, S. R., Nair, K. N. V., & Nair, S. R. S. (1994). Oil sardine and Indian mackerel: Their fishery, problems and coastal oceanography. *Current Science*, 66(5), 340–348.

Manjusha, U., Jayasankar, J., Remya, R., Ambrose, T. V., & Vivekanandan, E. (2013). Influence of coastal upwelling on the fishery of small pelagics off Kerala, south-west coast of India. *Indian Journal of Fisheries*, 60(2), 37–42.

McClatchie, S. (2014). *Regional fisheries oceanography of the California Current System. The CalCOFI Program.* Dordrecht: Springer. https://doi.org/10.1007/978-94-007-7223-6

McClatchie, S., Goericke, R., Auad, G., & Hill, K. (2010). Re-assessment of the stock–recruit and temperature–recruit relationships for Pacific sardine (*Sardinops sagax*). *Canadian Journal of Fisheries and Aquatic Sciences*, 67(11), 1782–1790. https://doi.org/10.1139/F10-101

Mendelssohn, R. (1981). Using Box-Jenkins models to forecast fishery dynamics: Identification, estimation and checking. *Fishery Bulletin*, 78(4), 887–896.

Menon, N. N., Sankar, S., Smitha, A., George, G., Shalin, S., Sathyendranath, S., & Platt, T. (2019). Satellite chlorophyll concentration as an aid to understanding the dynamics of Indian oil sardine in the southeastern Arabian Sea. *Marine Ecology Progress Series*, 617–618, 137–147. https://doi.org/10.3354/meps12806

Moustahfid, H., Marsac, F., & Grangopadhyay, A. (2018). Climate change impacts, vulnerabilities and adaptations: Western Indian Ocean marine fisheries. In M. Barange, T. Bahri, M. C. M. Beveridge, K.

L. Cochrane, S. Funge-Smith, & F. Poulain (Eds.), *Impacts of climate change on fisheries and aquaculture: Synthesis of current knowledge, adaptation and mitigation options* (pp. 251–280). : FAO Fisheries; Aquaculture Technical Paper No. 627.

Murty, A. V. S., & Edelman, M. S. (1966). On the relation between the intensity of the south-west monsoon and the oil-sardine fishery of India. *Indian Journal of Fisheries*, 13(1/2), 142–149.

Naidu, P. D., Kumar, M. R. R., & Babu, V. R. (1999). Time and space variations of monsoonal upwelling along the west and east coasts of India. *Continental Shelf Research*, 19(4), 559–572. https://doi.org/10.1016/S0278-4343(98)00104-6

Nair, P. G., Joseph, S., Kripa, V., Remya, R., & Pillai, V. N. (2016). Growth and maturity of Indian oil sardine *Sardinella longiceps* (Valenciennes, 1847) along southwest coast of India. *Journal of Marine Biological Association of India*, 58(1), 64–68. https://doi.org/10.6024/jmbai.2016.58.1.1899-07

Nair, R. V. (1952). Studies on the revival of the Indian oil sardine fishery. *Proceedings of Indo-Pacific Fisheries Council*, 2, 1–15.

Nair, R. V. (1959). Notes on the spawning habits and early life-history of the oil sardine, *Sardinella longiceps* Cuv. & Val. *Indian Journal of Fisheries*, 6(2), 342–359.

Nair, R. V., & Subrahmanyan, R. (1955). The diatom, *Fragilaria oceanica* Cleve, an indicator of abundance of the Indian oil sardine, *Sardinella longiceps* Cuv. and Val. *Current Science*, 24(2), 41–42.

Nobel, A., & Sathianandan, T. V. (1991). Trend analysis in all-India mackerel catches using ARIMA models. *Indian Journal of Fisheries*, 38(2), 119–122.

Pillai, V. N. (1991). Salinity and thermal characteristics of the coastal waters off southwest coast of India and their relation to major pelagic fisheries of the region. *Journal of the Marine Biological Association of India*, 33(1/2), 115–133.

Piontkovski, S., Al Oufi, H., & Al Jufaily, S. (2014). Seasonal and inter-annual changes of Indian oil sardine, *Sardinella longiceps*, landings in the governorate of Muscat (the Sea of Oman). *Marine Fisheries Review*, 76(3), 50–59. https://doi.org/10.7755/MFR.76.3.3

Pitchaikani, J. S., & Lipton, A. P. (2012). Impact of environmental variables on pelagic fish landings: Special emphasis on Indian oil sardine off Tiruchendur coast, Gulf of Mannar. *Journal of Oceanography and Marine Science*, 3(3), 56–67. https://doi.org/10.5897/JOMS

Prabhu, M. S., & Dhulkhed, M. H. (1970). The oil sardine fishery in the Mangalore zone during the seasons 1963–64 and 1967–68. *Indian Journal of Fisheries*, 17(1/2), 57–75.

Prista, N., Diawara, N., Costa, M. J., & Jones, C. (2011). Use of SARIMA models to assess data-poor fisheries: A case study with a sciaenid fishery off Portugal. *Fisheries Bulletin*, 109(2), 170–185. https://doi.org/10.7755/FB

R Development Core Team (2019). *R: A language and environment for statistical computing*. Vienna, Austria: R Foundation for Statistical Computing. https://www.R-project.org/

Rao, A. D., Joshi, M., & Ravichandran, M. (2008). Oceanic upwelling and downwelling processes in waters off the west coast of India. *Ocean Dynamics*, 58(3/4), 213–226. https://doi.org/10.1007/s10236-008-0147-4

Rohit, P., Sivadas, M., Abdussamad, E. M., Rethinam, A. M. M., Koya, K. P. S., Ganga, U., Supraba, V. (2018). *Enigmatic Indian oil sardine: An insight*. CMFRI Special Publication No. 130. p156. ICAR-Central Marine Fisheries Research Institute.

Roxy, M. K., Ritika, K., Terray, P., & Masson, S. (2014). The curious case of Indian Ocean warming. *Journal of Climate*, 27(22), 8501–8509. https://doi.org/10.1175/JCLI-D-14-00471.1

Rykaczewski, R. R., & Checkley, D. M. Jr (2008). Influence of ocean winds of the pelagic ecosystem in upwelling regions. *Proceedings of the National Academy of Science*, 105(6), 1965–1970. https://doi.org/10.1073/pnas.0711777105

Sajna, V. H., Zacharia, P. U., Liya, V. B., Rojith, G., Somy, K., Joseph, D., & Grinson, G. (2019). Effect of climatic variability on the fishery of

Indian oil sardine along Kerala coast. *Journal of Coastal Research*, *86*(sp1), 184–192. https://doi.org/10.2112/SI86-028.1

Schaaf, W. E., Sykes, J. E., & Chapoton, R. B. (1975). Forecasts of Atlantic and Gulf menhaden catches based on the historical relation of catch and fishing effort. *Marine Fisheries Review*, *37*(10), 5–9. https://doi.org/10.7755/MFR

Schwartzlose, R. A., Alheit, J., Bakun, A., Baumgartner, T. R., Cloete, R., Crawford, R. J. M., Fletcher, W. J., Green-Ruiz, Y., Hagen, E., Kawasaki, T., Lluch-Belda, D., Lluch-Cota, S. E., MacCall, A. D., Matsuura, Y., Nevárez-Martínez, M. O., Parrish, R. H., Roy, C., Serra, R., Shust, K. V., ... Zuzunaga, J. Z. (2010). Worldwide large-scale fluctuations of sardine and anchovy populations. *South African Journal of Marine Science*, *21*(1), 289–347. https://doi.org/10.2989/025776199784125962

Schwing, F. B., O'Farrell, M., Steger, J., & Baltz, K. (1996). Coastal upwelling indices, west coast of North America 1946–1995. NOAA Technical Memorandum NMFS-SWFSC-231.

Shafeeque, M., Shah, P., Platt, T., Sathyendranath, S., Menon, N. N., Balchand, A. N., & George, G. (2019). Effect of precipitation on chlorophyll-a in an upwelling dominated region along the West coast of India. *Journal of Coastal Research*, *86*(sp1), 218–224. https://doi.org/10.2112/SI86-032.1

Shah, P., Sajeev, R., Thara, K. J., George, G., Shafeeque, M., Akash, S., & Platt, T. (2019). A holistic approach to upwelling and downwelling along the South-West coast of India. *Marine Geodesy*, *42*(1), 64–84. https://doi.org/10.1080/01490419.2018.1553805

Srinath, M. (1998). Exploratory analysis on the predictability of oil sardine landings in Kerala. *Indian Journal of Fisheries*, *45*(4), 363–374.

Srinath, M., Kuriakose, S., & Mini, K. G. (2005). *Methodology for estimation of marine fish landings in India*. In *CMFRI Special Publications No. 86. p57*. Central Marine Fisheries Research Institute.

Stergiou, K. I., & Christou, E. D. (1996). Modelling and forecasting annual fisheries catches: Comparison of regression, univariate and multivariate time series methods. *Fisheries Research*, *25*(2), 105–138. https://doi.org/10.1016/0165-7836(95)00389-4

Supraba, V., Dineshbabu, A. P., Thomas, S., Rohit, P., Rajesh, K. M., & Zacharia, P. U. (2016). Climate influence on oil sardine and Indian mackerel in southeastern Arabian Sea. *International Journal of Development Research*, *6*(8), 9152–9159.

Thara, K. J. (2011). *Response of eastern Arabian Sea to extreme climatic events with special reference to selected pelagic fishes*. Kerala, India: PhD Thesis. Department of Physical Oceanography. Cochin University of Science and Technology.

Tommasi, D., Stock, C. A., Pegion, K., Vecchi, G. A., Methot, R. D., Alexander, M. A., & Checkley, D. M. Jr (2016). Improved management of small pelagic fisheries through seasonal climate prediction. *Ecological Applications*, *27*(2), 378–388. https://doi.org/10.1002/eap.1458

Vallivattathillam, P., Iyyappan, S., Lengaigne, M., Ethé, C., Vialard, J., Levy, M., Suresh, N., Aumont, O., Resplandy, L., Naik, H., & Naqvi, W. (2017). Positive Indian Ocean Dipole events prevent anoxia off the west coast of India. *Biogeosciences*, *14*(6), 1541–1559. https://doi.org/10.5194/bg-14-1541-2017

Venugopalan, R., & Srinath, M. (1998). Modelling and forecasting fish catches: Comparison of regression, univariate and multivariate time series methods. *Indian Journal of Fisheries*, *45*(3), 227–237.

Vivekanandan, E., Rajagopalan, M., & Pillai, N. G. K. (2009). Recent trends in sea surface temperature and its impact on oil sardine. In P. K. Aggarwal (Ed.), *Global climate change and Indian agriculture* (pp. 89–92). Indian Council of Agricultural Research.

Vivekanandan, E., Srinath, M., Pillai, V. N., Immanuel, S., Kurup, K. N., 2003). Marine fisheries along the southwest coast of India. In G. Silvestre, L. Garces, I. Stobutzki, C. Luna, M. Ahmad, R. A. Valmonte-Santos, & D. Pauly (Eds.), *Assessment, management, and future directions for coastal fisheries in Asian countries* (pp. 759–792). WorldFish Center, Penang.: WorldFish Center Conference Proceedings 67.

Ward, E. J., Holmes, E. E., Thorson, J. T., & Collen, B. (2014). Complexity is costly: a meta-analysis of parametric and non-parametric methods for short-term population forecasting. *Oikos*, *123*(6), 652–661. https://doi.org/10.1111/j.1600-0706.2014.00916.x

Wood, S. N. (2011). Fast stable restricted maximum likelihood and marginal likelihood estimation of semiparametric generalized linear models. *Journal of the Royal Statistical Society B*, *73*(1), 3–36. https://doi.org/10.1111/j.1467-9868.2010.00749.x

Wood, S. N. (2017). *Generalized additive models: An introduction with R*. CRC Press. https://doi.org/10.1201/9781315370279

Xu, C., & Boyce, M. S. (2009). Oil sardine (*Sardinella longiceps*) off the Malabar coast: Density dependence and environmental effects. *Fisheries Oceanography*, *18*(5), 359–370. https://doi.org/10.1111/j.1365-2419.2009.00518.x

Zhang, R., & Delworth, T. L. (2006). Impact of Atlantic multidecadal oscillations on India/Sahel rainfall and Atlantic hurricanes. *Geophysical Research Letters*, *33*(17), L17712. https://doi.org/10.1029/2006GL026267

Zhang, R., Sutton, R., Danabasoglu, G., Kwon, Y.-O., Marsh, R., Yeager, S. G., Amrhein, D. E., & Little, C. M. (2019). A review of the role of the Atlantic Meridional Overturning Circulation in Atlantic Multidecadal Variability and associated climate impacts. *Reviews of Geophysics*, *57*(2), 316–375. https://doi.org/10.1029/2019RG000644

SUPPORTING INFORMATION

Additional supporting information may be found online in the Supporting Information section.